Superfluidity and Random Media

by

Hsin-Fei Meng

B.S., National Taiwan University (1987)

Submitted to the Department of Mathematics
in partial fulfillment of the requirements for the degree of

Doctor of Philosophy

at the

MASSACHUSETTS INSTITUTE OF TECHNOLOGY

June 1993

© Massachusetts Institute of Technology

Signature of Author . . . . Signature redacted . . . .
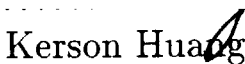
Department of Mathematics
April 30, 1993

Certified by . . . . Signature redacted . . . .

Hung Cheng   Kerson Huang

Professor of Applied Mathematics   Professor of Physics

Thesis Supervisor

Accepted by . . . . Signature redacted . . . .

Sigurdur Helgason

Chairman, Departmental Graduate Committee

Department of Mathematics

Superfluidity and Random Media

by

Hsin-Fei Meng

Abstract

This Thesis contains a theoretical study of the disordered boson system. The most important property of pure interacting boson system at low temperature is superfluidity. In order to understand various phenomena in the real world where some amount of disorder is always present, it is natural to study the effect of the randomness on superfluidity. This problem has the well-known difficulty that, unlike the corresponding electron system, the self-interaction can not be treated as a perturbation. This is because without the self-interaction the whole system will collapse and becomes a state far different from the physical systems which we intend to study. In this Thesis both microscopic and phenomenological approaches are used to study this long-standing problem.

In chapter one I give a general account of the experimental situations and theoretical bases. In chapter two I will report the results on the Bogoliubov theory of liquid helium including weak external random potential. It is shown that superfluidity could be destroyed when the total liquid density is too small. It demonstrates that disorder can in fact change the qualitative nature of the system. In chapter three I will study the corresponding two dimensional system with a new method. It turns out that our method has a direct application to the interesting problems of fractional quantum Hall effect. Numerical results on the strongly disordered superfluid will also be discussed. Chapter four is a model to explain one of the most striking experiments regarding disordered helium: the superfluid transition on porous media. Almost all the experimental observations can be understood within this model.

CONTENT

Chapter 4   Superfluid Helium in Disordered Media at Full Pore

Chapter One

Introduction

1.1 Physical Properties of Liquid Helium

Liquid helium is usually referred to as a kind of "quantum liquid", due to the fact that very few of its thermodynamical and fluid-dynamical properties can be understood in terms of classical physics. This is perhaps the reason it has received enormous theoretical and experimental study since its discovery. Despite the great amount of efforts already been made, the physics of liquid helium is far from being completely understood. For example, nobody knows how to derive the λ-transition critical index from a microscopic model. In this section I will discuss some experiments on the properties of liquid helium that bear relevance to the theoretical studys in the following chapters.

Helium has two isotopes, ^{4}He and ^{3}He. The low temperature phase diagrams of these two species are quite different. In particular, ^{4}He becomes the so-called superfluid when the temperature is lower than 2.17 K while ^{3}He remains a normal fluid until about 3×10^{-3} K. One should not be surprised by this difference as ^{4}He is a boson while ^{3}He is a fermion. In the following I will consider ^{4}He only. The problem of ^{3}He is a totally different subject. Without explicit reference the term helium will simply mean ^{4}He.

The boiling point of helium 4.21 K is the lowest of all substances. If the temperature is further lowered, it experiences a phase transition at about 2.17 K. This transition is usually referred to as λ-transition and the transition temperature is called T_λ. Above T_λ

the liquid behaves like a normal viscous fluid. Below T_λ many surprising new properties show up. They are in general referred to as the properties of a *superfluid*. Accompanied with the normal fluid-superfluid transition is a sharp singularity of the specific heat at T_λ. The temperature dependence of specific heat is shown in figure 1.1 [1] . The shape of the curve resembles the Greek letter λ, hence the name of the transition. The singularity is believed to be logrithmic. The transition is very "pure" in the sense that the singularity does not get rounded up even in extremely narrow temperature range. Under normal pressure it is believed that the system remains a liquid down to absolute zero temperature.

One of the best way to demonstrate the superfluid property is the Andronikashvili's experiment which is schematically shown in figure 1.2 . When the pile of discs rotates, only a portion of the fluid is dragged along. The spacing of the discs is so small that above T_λ all the fluid is dragged along. So in a superfluid a fraction of the fluid is inert to the external dragging force. In other words, they are not viscous at all. This lack of viscosity can be further illustrated by the experiments related to the *superleak* (figure 1.3). In a channel with diameter as narrow as about 100 nm liquid helium can flow through when there is a temperature difference at the two ends. A viscous normal fluid can never leak through such a narrow channel.

The above two examples include only one side of the meanings of *superfluidity*. Superfluidity has a two-fold meaning. It could mean the inertia of the fluid to external dragging force, or it could mean the existence of a *persistent superflow.*
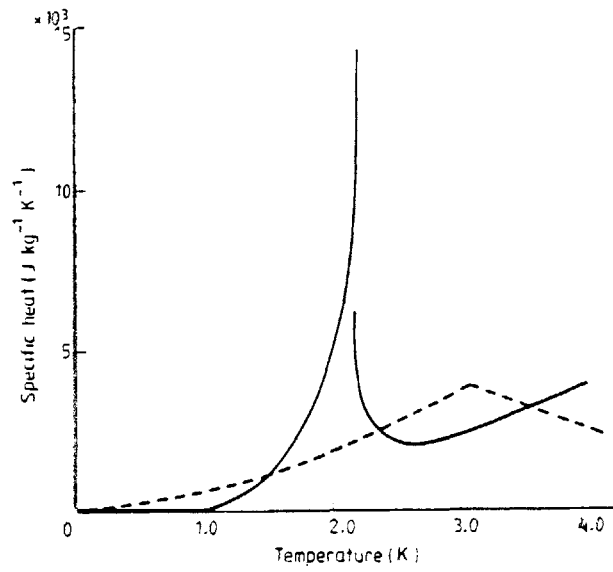
Fig. 1.1

Sepecific heat of liquid ^{4}helium. Broken line shows the specific heat of idel bose gas having the same

density as ^{4}He. See P.4 of Ref.1
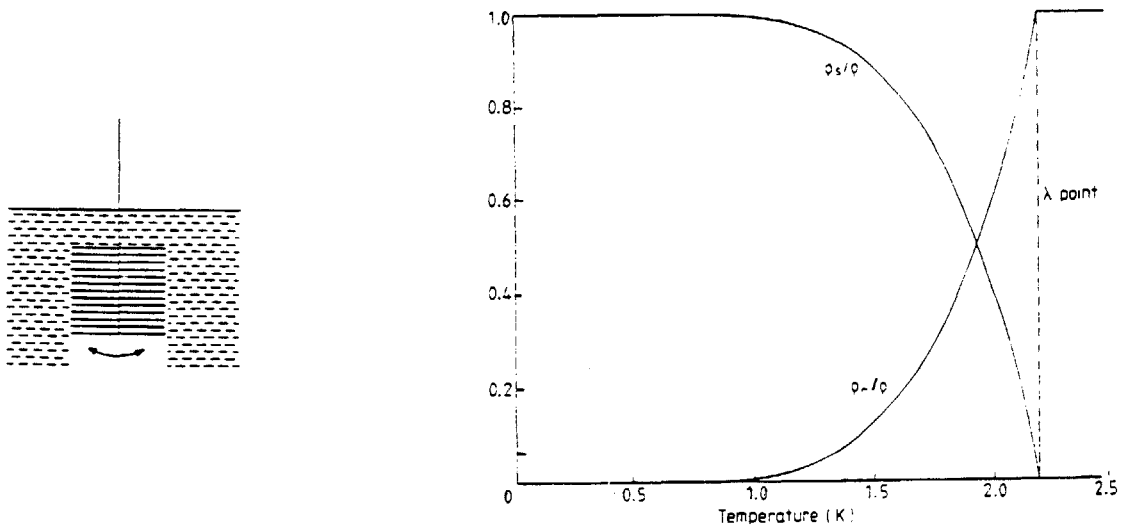
Fig. 1.2

Andronikashivili's experiment

3

Fig. 1.3

Two vessels connected by a superleak. A temperature difference between the two is accompanied by a presuure head. See P.9 of Ref.1

In the experiment of Reppy and Depatie [2] an initial current of liquid helium is set up in a torus when the temperature is above T_λ. After the whole thing is cooled down below T_λ, the liquid inside can flow around the torus indefinitely. No angular velocity decay is detected over a twelve-hour period. The theoretical version of this persistent superflow is that the flowing state is in fact a *Hamiltonian eigenstate*. It is obviously not the ground state since it carries a lot of energy. However, the transition to the ground state is prohibited by the energy barrier. In other words, it is a *metastable state*. These two pictures of superfluidity are actually equivalent to each other. This point will be explained later after the mathematical definition of the superfluid is formulated.

The phase diagram of ^{4}He can be found in many text books [3]. The purpose of this

thesis is not to explain the physics of the various phases. Instead, it is a theoretical study of how the liquid behaves in the presence of disorder, or impurities, especially in the low temperature region.

1.2 Mathematical Definition of a Superfluid

Since superfluidity is primarily a experimental phenomenon. I will take an operational definition which bear a close relation to what happens in the real experiments. Consider an infinitely long pipe filled with helium, both the pipe and the liquid are brought to complete rest at t(time)$= -\infty$. Let's then accelerate the wall infinitely slowly. After an infinite amount of time the velocity of the wall at $t = 0$ becomes v. *Normal fluid density* ρ_n is defined to be the fraction of the fluid that is moved along with the wall after this process. In other words, the momentum density $< g >$ at $t = 0$ and ρ_n are related by

$$< g > \equiv \rho_n v \tag{1}$$

The *superfluid density* ρ_s is simply the difference between the total density ρ and the normal fluid density.

$$\rho_s \equiv \rho - \rho_n \tag{2}$$

See figure 1.4 .

One may ask a nature question: How does the wall interact with the fluid in parctice? Of course the answer depends on the kind of wall we are using. However it will be shown later that the *detailed form* of the interaction has no effect on the results. So the value of the superfluid density will not change with the choice of the wall.

t = minus infinity

velocity=0

hard wall

liquid helium

t = zero

wall velocity = v

fluid momentum density =
normal density x v
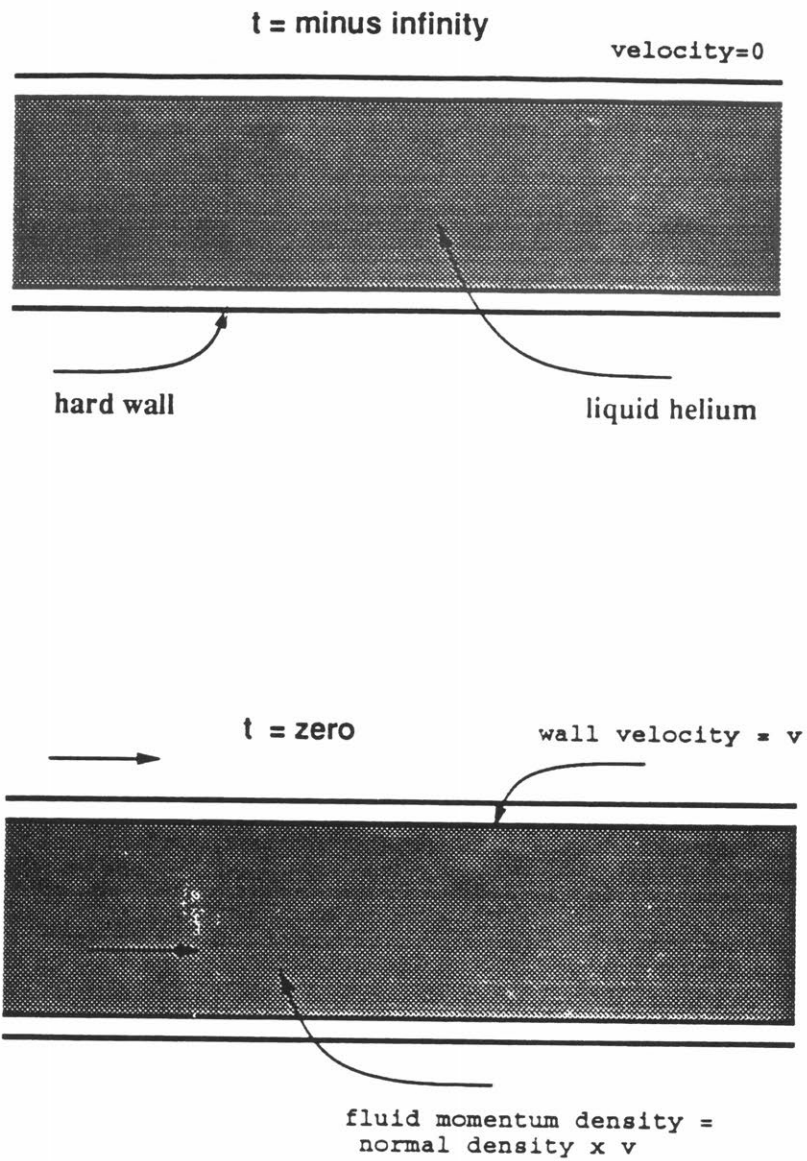
Fig. 1.4

The operational definition of ρ_s. At $t = -\infty$ the whole thing is brought to complete rest. The wall is accelerated adaibatically from rest to velocity v. The fraction of fluid that is dragged along is the normal fluid part.

It should be noticed that even though there is an apparent reference to the wall in the definition, superfluid density ρ_s is an *internal property* of the liquid and could be expressed without the wall also. This is actually what I will do in the following.

Let's consider a more general case now. Instead of a moving wall, we can turn on a external force field $\vec{v}(x, t)$ infinitely slowly. The effect of the external field is described by the interaction Hamiltonian

$$H_I = - \int d^3x \, \vec{g}(x) \cdot \vec{v}(x, t) \, ,$$

where $\vec{g}$ is the momentum density. Moving wall just corresponds to some particular choice of $\vec{v}$. I will come back to this connection after considering the response of the liquid to a general $\vec{v}(x, t)$. The linear response is given by the Kubo formula :

$$< g_i(x, t) > = \int_{-\infty}^{\infty} ds \int d^3y \, \chi_{ij}(x, t; y, s) v_j(y, s) \tag{3}$$

with

$$\chi_{ij}(x, t; y, s) \equiv i\theta(t - s) < [g_i(x, t), g_j(y, s)] >$$

The behavior of the momentum density correlation function is central to the definition of superfluidity.

Since the space-time is homogeneous, $\chi_{ij}(x, t; y, s)$ is of the form $\chi_{ij}(x - y, t - s)$. The Fourier transform of $\chi_{ij}(x - y, t - s)$ is $\chi_{ij}(k, \omega)$. If we turn on the external field infinite slowly, the time dependence of $\vec{v}$ can be taken to be

$$\vec{v}(x, t) = \vec{v}(x)e^{\epsilon t} \, , \quad -\infty < t < 0$$

7

where ϵ is an infinitesimal quantity. We are interested in the values of the physical quantities at $t = 0$ after this long process. For this purpose let's define the *static response function* $\chi_{ij}(x)$

$$\chi_{ij}(x) \equiv \int_{-\infty}^{0} \chi_{ij}(x,t)e^{\epsilon t}dt$$

The Fourier transform of it is

$$\widetilde{\chi}_{ij}(k) = \int_{-\infty}^{\infty} \frac{d\omega}{2\pi} \frac{\chi(k,\omega)}{\omega + i\epsilon}$$

At $t = 0$ we have

$$< g_i(k) > = \widetilde{\chi}_{ij}(k)v_j(k)$$

where $\vec{v}(k)$ is the Fourier transform of $\vec{v}(x)$. Since $\widetilde{\chi}_{ij}(k)$ is a second rank tensor, it has to be of the form

$$\widetilde{\chi}_{ij}(k) = \frac{k^i k^j}{k^2}A(k) + \delta^{ij}B(k) \tag{4}$$

where A and B are functions of the magnitude of k only. In terms of A and B, the linear response relation becomes

$$< g_i(k) > = A(k)\frac{\vec{k} \cdot \vec{v}(k)}{k^2}k^i + B(k)v_i(k) \tag{5}$$

It's time for us to come back to the moving wall now. The interaction between the wall and the liquid must happen in a short but finite range along the wall surface. The strength of the dragging force is a sharply peaked function around the contact face. Deep inside the liquid there should be no force at all. Since the the wall is translationally invariant, the force changes only in the normal direction of the surface. As for the direction, it's clear that the field is always in the moving direction, which is perpendicular to the normal

8

direction. So $\vec{v}(\vec{k})$ is nonvanishing only when $\vec{k}$ is in the normal direction, however $\vec{v}(\vec{k})$ itself is always perpendicular to it. In other words

$$\vec{k} \cdot \vec{v}(\vec{k}) = 0$$

Thus we conclude that the dragging force is always transverse. So the first part of eq.(1.5) will never contribute and we get $g_i(k) = B(k)v_i(k)$.

Now we have related the final momentum density distribution with the applied external field. The next question is how to relate the force field $\vec{v}(k)$ with the final velocity v which appear in the very beginning of the definition of ρ_s. In order to accomplish this let's consider a classical, or normal fluid first. It can be shown that for a classical fluid we have [3]:

$$\widetilde{\chi}_{ij}(k) = \delta^{ij}\rho \quad , \quad (classical\ fluid)$$

where ρ is the total mass density. As a result, a force field $\vec{v}(k)$ is applied to a classical fluid the final momentum distribution is $g_i(k) = \rho v_i(k)$, in particular

$$g_i(0) = \rho v_i(0) \tag{6a}$$

However, independently we know that if $\vec{v}$ is the dragging force, the final density should satisfy

$$g_i(0) = \rho v \tag{6b}$$

since the whole thing will move along the wall eventually for a classical fluid. Comparing eq.(1.6a) and eq.(1.6b) we conclude that

$$v_i(0) = v$$

9

In general, the same force field will result in the final momemtum

$$g_i(0) = B(0)v$$

So, by definition,

$$B(0) \equiv \rho_n \tag{7}$$

Furthermore, from one of the exact sum-rules we know [3]

$$A(0) + B(0) = \rho \ , \ (f - sum - rule) \tag{8}$$

Combine the above two equations we have

$$\rho_s \equiv \rho - \rho_n = A(0)$$

The liner response function is in fact

$$\widetilde{\chi}_{ij}(k) = \rho_s \frac{k^i k^j}{k^2} + \rho_n \delta^{ij} \tag{9}$$

Now we have reached a expression of the superfluid density free of the reference to any walls. It is expressed in terms of the equilibrium thermal average of certain operators. In contrast to thermodynamical quantities like energy and specific heat, it is an *dynamical coefficient* that determines how the system responds to certain external disturbances. In order to measure it we must apply some kind of external force to drive the system slightly out of equillibrium.

The mathematical definition of ρ_s is not a completely settled problem [4]. Different definitions appear in the literature. For example, in the famous paper by Nelson and Kosterlitz [5] on the universal jump of liquid helium thin film, they use a definition of ρ_s in

10

terms of the correlation function of the phase of the field operator. In that particular case, this two definitions just happen to agree with each other within the range of the validity of their theory.

A rigorous proof of the equivalence among the definitions does not seem to be possible. While not being able to do this I believe the definition presented above is the one most related to the experiments. In fact, in most cases, it *is* the quantity we measure in the experiments.

It is clear now that we can reconcile the two independent concepts of superfluidity mentioned the previous section, i.e. *inertia to external force* and *existence of persistent current*. When an adiabatical force is applied to the system the initial and final states should be eigenstates of the initial and final Hamiltonian respectively. Call the reference frame where the wall is at rest initially L1 and the frame moving with the wall finally L2. When $t = 0$ the state of the liquid in L1 is called $|H1>$. The momentum density of $|H1>$ is $\rho_n v$. The corresponding state seen in L2 is called $|H2>$. $|H2>$ should be an eigenstate of the Hamiltonian in L2, which is simply the one with a fixed wall. What is the momentum density of $|H2>$ seen in L2? By Galelien transformation it is $\rho v - \rho_n v = \rho_s v \neq 0$. Thus we find the state $|H2>$ with a persistent current. It is an eigenstate of Hamiltonian with fixed wall but carries a finite amount of momentum.

So far the super and normal fluid density are properties of the whole bulk by definition. However, in the so called hydrodynamical region they can be treated as functions of space and time. The equations that govern their evolution is called two-fluid hydrodynamical equations. It is called two-fluid because in the lowest order approximation we can assume

that there is no interaction between the super and normal components. In order to make such treatment sensible there must exist a length scale which is small enough such that the parameters like temperature and external fields are essentially constants within this scale but large enough such that the system is in local thermodynamical equilibrium and ρ_n, ρ_s can be defined locally.

1.3 Bogoliubov Theory of Liquid Helium

The most, perhaps only, successful microscopic first-principle model of liquid helium is first proposed by Bogoliubov [6] then Huang and Yang [7]. The detailed derivation can be found in many good references [8]. I won't bother to rederive them here. However I will discuss the assumptions made in this model and the some of the important results they got.

One of the facts that make liquid helium such an interesting quantum fluid is that ^{4}He atom is a boson. If there is no self-interaction, at zero temperature all the particles will stay in one single state: the ground state of the one-particle spectrum. In the homogeneous case it is the zero-momentum state. For the interacting system it's not sensible to talk about one-particle eigenstate, however the expectation value of the *occupation number* N_0 of one-particle zero-momentum state should still be a macroscopical quantity. It means in the thermodynamical limit N_0 is proportional to V, the system volume. This phenomenon is called bose condensation. $n_0 \equiv N_0/V$ is called the condensate density.

A nonvanishing n_0 can be also seen as a result of spontaneous symmetry breaking (SSB) in the interacting case. The microscopic Hamiltonian H of this interacting boson many-body system is

$$H = \int \frac{1}{2m} \vec{\nabla}\Psi^\dagger(x)\vec{\nabla}\Psi(x)d^dx - \mu \int \Psi^\dagger(x)\Psi(x)d^dx$$

$$+\frac{1}{2}\int \Psi^\dagger(x)\Psi^\dagger(y)v(x-y)\Psi(x)\Psi(y)d^dxd^dy \tag{10}$$

with

$$[\Psi(r), \Psi^\dagger(r')] = \delta(r - r')$$

13

μ is the chemical potential, m is the helium atom mass. $V(x)$ is the short-ranged hard core self-interaction between helium atoms and can be replaced by a delta function $v_0 \delta(x)$ [7]. v_0 is equal to $4\pi a/m$, where a is the hard sphere diameter. The Hamiltonian becomes

$$H = \int \frac{1}{2m} \vec{\nabla} \Psi^\dagger \vec{\nabla} \Psi d^3 x - \mu \int \Psi^\dagger \Psi d^d x + \frac{1}{2} v_0 \int \Psi^\dagger \Psi^\dagger \Psi \Psi d^3 x$$

Let's concentrate on the ground state of H for the moment. If Ψ is a c-number instead of an operator then this answer is easy. The Ψ that minimizes the energy is simply $\sqrt{\mu/v_0}$ times a pure phase factor. The phase θ can be anything between 0 and 2π. Obviously, a phase factor change in Ψ leaves the Hamitonian unchanged. We say H has an U(1) symmetry. However the ground state does not possess this symmetry since under the transformation

$$\sqrt{\frac{\mu}{v_0}} \rightarrow \sqrt{\frac{\mu}{v_0}} e^{-i\theta} \neq \sqrt{\frac{\mu}{v_0}}$$

In general, we call the situation that the symmetry of the Hamiltonian is not shared by the ground state SSP. In the quantum level, we *expect* the same thing to happen. That is

$$< \Psi > \neq 0$$

The value of $< \Psi >$ is in general different from the corresponding classical value due to the so called *radiative correction*. However, as long as $< \Psi >$ is not zero, the symmetry broken. What is the symmetry now? The generator of the symmetry group it now $\int d^3 \Psi^\dagger \Psi = N$. H is invariant under the transformation group generated by N:

$$H \rightarrow e^{-i\theta N} H e^{i\theta N} = H$$

This is obvious since H and N commute with each other. The fact $< \Psi >$ is not zero implies that the ground state, or vacuum, is not invariant under the transformation. This

14

can be easily seen since

$$e^{-i\theta N}\Psi e^{i\theta N} = \Psi e^{-i\theta}$$

If the vacuum $|0>$ is invariant under the transformation, when sandwitched between $<0|$ and $|0>$ the above equation gives

$$<\Psi> = <\Psi> e^{-i\theta}$$

This contradicts with the assumption that $<\Psi>$ is nonzero.

One might be curious about what kind of nature of the vacuum causes the SSB. The answer is that *the bose condensation makes the spontaneous symmetry breaking possible.* If we take the base of the many-body Hilbert space to be the direct products of the one-particle momentum eigenstates, then the vacuum $|0>$ will be a linear combination of states with different zero-momentum occupation numbers. In other words, they are eigenstates of $a_0^\dagger a_0$ with different eigenvalues, where a_0 is the annihilation operator of zero-momentum state. All of the eigenstates are macroscopically large. From

$$a_0|N> = \sqrt{N}|N-1> \ , \ a_0^\dagger|N> = \sqrt{N+1}|N+1>$$

It is easy to see that if $|0>$ is composed of states with N's highly concentrated on the large mean value N_0 then $|0>$ has the property

$$a_0|0> \simeq a_0^\dagger|0> \simeq \sqrt{N_0}|0> \ , \ <0|\Psi|0> \simeq \sqrt{n_0} \tag{11}$$

with $n_0 = N_0/V$. So the vacuum is almost an eigenstate of the creation and annihilation operators of the zero-momentum state. This is the basic starting point of the Bogoliubov

15

model. Let's define a new Hamiltonian H_B obtained from H by replacing all the a_0 and $a_0^\dagger$ by $\sqrt{N_0}$. We have

$$H_B|0> \simeq H|0> \tag{12}$$

This is in fact true not only for the ground state but for all the eigenstates with zero-momentum occupation around N_0. Thus the low-lying eigenstates of H_B should be a good approximation to the corresponding ones of H. This replacement greatly simplifies the problem. In fact it turns an intractable one into a tractable one. After throwing away some higher order terms, H_B can be diagonized by the so-called Bogoliubov transformation which is the technique we will use in the second chapter.

One of the most important predictions of this model is that the dispersion relation of the elementary excitation ω_p is linear when the momentum p is small. In fact we have

$$\omega_p = cp \tag{13}$$

where c is the sound velocity. It turns out that this linear dispersion relation is crucial to the fact that liquid helium is a superfluid. One can hardly find a more brilliant way to demonstrate this than the classical argument by Landau [9]. He showed that when the velocity of moving wall is less than some critical value, it's impossible to cause any excitation to the fluid. The only assumptions he used in the argument are the linear spectrum and the Galelien invariance.

In fact, most of the low-temperature properties of liquid helium can be well explained by the Bogoliubov model. However it begins to break down when one needs to consider states far away from the vacuum. For example, it can not explain the roton part of the spectrum at higher momentums (Figure 1.5). Furthermore, the λ-transition is completely

out of the scope of this model. The excitations that govern the physics of λ-transition is believed to be the vortices which are absent in the Bogoliubov model.

In addition to thermal fluctuations like phonons and vortices, another factor to reduce the superfluid density is the presence of disorder. In fact, in the case of strong disorder the nature of the super-normal fluid transition could be quite different from the case of pure helium. The effect of disorder on superfluidity will be the subject of the following chapters.
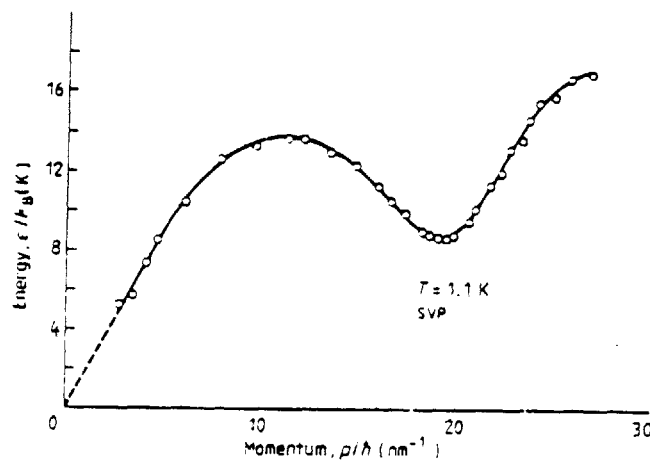

Fig. 1.5

The elementary excitation spectrum of liquid helium. In low momentum region there are phonons while in intermediate momentum region we have rotons which can no be derived from Bogoliubov theory.

The above consideration is for three dimensional (3D) systems only. In the corresponding 2D system there is no condensate at any finite temperature. Thus all the prerequisites of the Bogoliubov model become invalid. The interesting thing is that even though the low temperature theory for 2D system looks more complicated, there is a rather satisfactory theory of the super-normal fluid transitions [10] for helium thin films, while a similar theory for the 3D λ-transition has not been achieved even in the phenomenological level. I will present a new approach to the problem of 2D boson system in chapter three, where the Hamiltonian is diagonized in terms of the density and phase operators. It is, of course, valid only at the low temperature region as the Bogoliubov model.

1.4 Experimental Situations on Disordered Superfluid

The study of the disordered fermion systems has a rather long history. In addition to the continuous intensive experimental studies, a lot of theories have also been formulated [11]. However, much less is known about the corresponding disordered boson system. One of the reasons is that the electron systems in the natural all experience some degree of disorder or impurities. In metals or semiconductors the crystal lattice can never be perfect. As a result, the electrons experience a periodical potential from a perfect lattice plus a random potential caused by the defects. Those unavoidable defects are generally treated as a small perturbation. However we can also easily find examples of strong disorder for fermions, for example, the amorphous semiconductors and random alloys. As a reasonable first approximation, we can neglect the Coulumb interaction among the electrons and treat them as free particles moving in an external potential. The most important effect of disorder is the localization of some of the free electron eigenstates. The spectrum is

18

divided into regions of extended states and localized states. They are separated by the so called mobility edge. When the fermi level passes through the edge, the system transfers from an insulator to a conductor, or vise versa.

Bearing the situation of fermions in mind, let's look at the boson case. First one would ask: What are the physical systems of disordered bosons in the natural? I will consider the 2D and 3D cases separately.

For the 2D case, the helium thin film adsorbed on the substrate surface is the most obvious example. The surface can never be a perfectly smooth plane. It is at best a periodic array of atoms. The surface roughness is the measure of the strength of the disorder. Another more complicated example is the helium film adsorbed on the inner surface of porous media like Vycor and xerogel. The properties of the porous media will be discussed later. There has been a great amount of experiments on helium in the porous media recently [12]. The most interesting thing observed is that there is no superfluidity when the helium surface density is smaller than some critical value (see figure 1.6), which is true for both plane substrate and porous media. Intuitively we can understand this phenomenon in the following way. When we add the first layer of helium atoms they get trapped by the localization centers, or the potential wells, on the surface caused by the disorder. They thus form an immobile layer. When we add more atoms to the surface, the hilly potential landscape is screened out by the presence of the first layer. So the second layer becomes a superfluid. So do the other layers added after this. Pictorially the structure of the helium film is shown is figure 1.7.
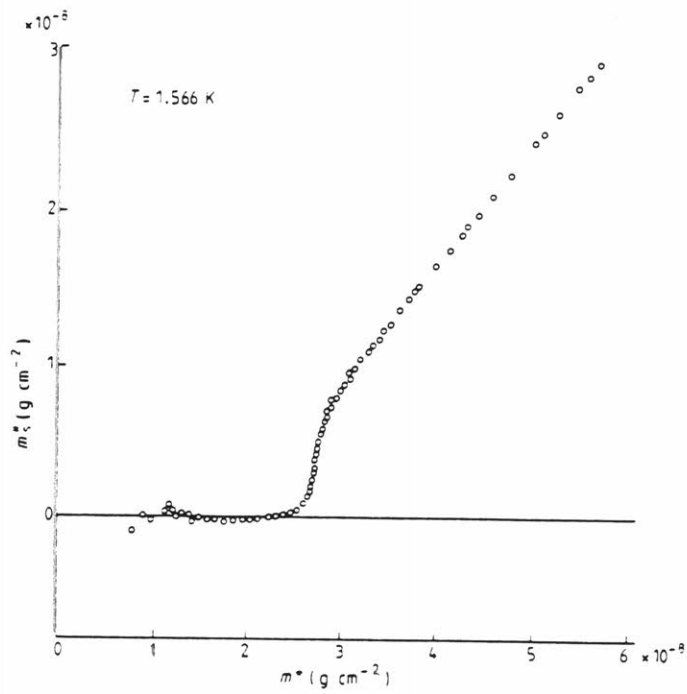
Fig. 1.6

Superfluid content (m_s^* = mass of superfluid per unit area) of helium film as a function of m^*, total mass of helium adsorbed per unit area. See P.103 of Ref.1
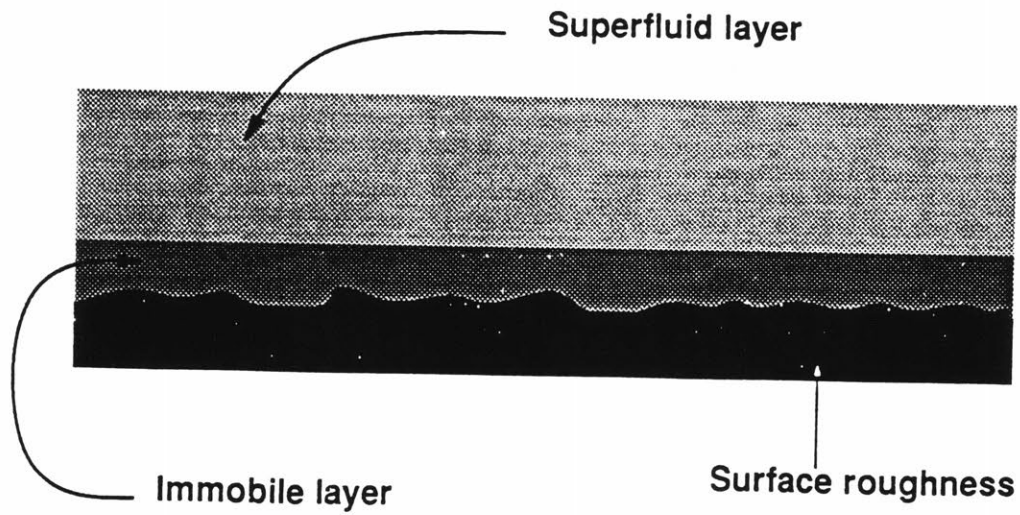

Fig. 1.7

Schematical structure of helium thin film adsorbed on a surface

The theoretical formulation of this situation is clearly very complicated. It is neither purely two dimensional nor purely three dimensional. Chapter three will be devoted to the development of a microscopic model for helium thin films in the presence of disorder.

Let's now turn to the 3D case. Obviously there is no unavoidable impurity present in the bulk liquid helium. In fact, it is one of the purest things we can prepare. However, physicists can always find ways to keep themselves busy by introducing the disorder artificially. The most conspicuous example of disordered 3D superfluid is perhaps the helium-filled porous media [13]. Before we go on, it's time to digress a little to discuss the properties of the porous media.

In general, porous medium is a medium with globally interconnected flow channels. Those channels are called pores. For *Vycor* (shown in figure 1.8 [14]), the pore diameters are roughly fixed around 10 nm, the open fraction (porosity) is about 30%. *Xerogel* has also pore diameters fixed around 10nm, but it differs from Vycor in that the channels are composed of a lot of dead ends. The structure of xerogel is similar to a percolation cluster which is highly ramified. The porosity of xerogel is about 60%. The last class of porous media considered here is *Aerogel*. Aerogel is a very delicate and dilute material. It has open fraction varying from 94% to more than 99%. It is believed to be fractal based on the neutron scattering experiments [15]. The pore sizes span over a very wide range, roughly from 0 to 100 nm.

Obviously, the effect of the porous media on the helium inside is not weak in general. In fact, it is more like providing a complicated new *boundary condition* than an external random potential as the effect of lattice defects for the electrons. The only exception is

21

perhaps aerogel since it is very dilute in space. The general feature of superlfuid in porous media is shown in the phase diagram in figure 1.9 [14] .

Chapter four will be a simulation of the superflow in the porous media. Percolation is proposed to be the mechanism of the superfluid transition. Some of the experimental results are explained and interpreted. Chapter two will be a study of 3D bose gas in an external random potential. How reasonable it is a model for helium in the porous media is not very clear. However, at least it is a well-defined and general problem and could have applications on systems other than liquid helium. A brief study of the problem of *boson localization* will be at the end of chapter three.

Fig. 1.8

Transmission electron micrograph of a thin section (about 350 Å) of Vycor. The micrograph shows that Vycor consists of a homogeneous and isotropic distribution of pores (dark areas) and glass (light areas). (Photo from P. Levitz, G. Ehret, J. M. Drake. Exxon Research and Engineering Company preprint.)

SUPERFLUID DENSITY (ρ_s)

$T = 0$

Filled Pores

COVERAGE

TEMPERATURE (T)
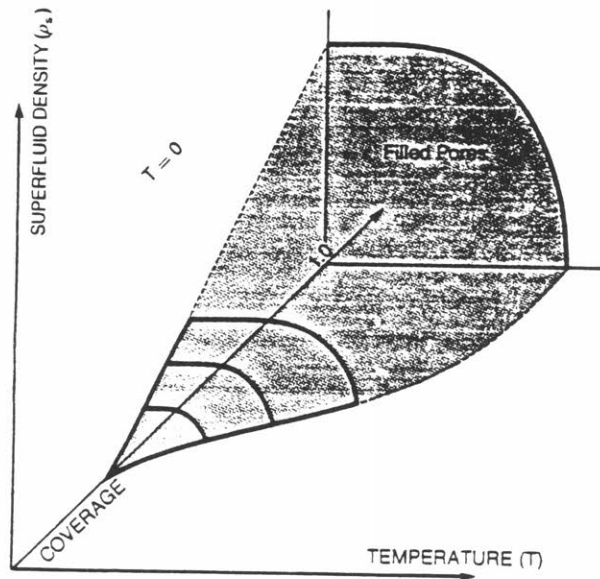
Fig. 1.9

Phase diagram of helium in Vycor, a porous medium. At $T = 0$ there is a phase transition to superfluidity at a nonzero value of coverage, measured here as a fraction of the helium density needed to *fill* the pores. This is in contrast with the behavior of pure, bulk helium, which is superfluid at $T = 0$ for all densities. The superfluid density ρ_s increases below the critical temperature with a $\frac{2}{3}$ power except when the critical temperature is on the order of a few tens of millikelvins, in which case the exponent predicted in the "Bose glass" theory may apply. Good data exist for filled pores and for thin films (coverage near 0.3) only. (Adapted from data reported in ref. 4.)

References

[1] D. Tilley and J. Tilley, *Superfluidity and Superconductivity* , 2nd ed. (Adam Hilger Ltd, 1986)

[2] J.D. Reppy and D. Depatie, Phys. Rev. Lett. **12**, 187 (1964).

[3] D. Forster, *Hydrodynamic Fluctuations, Broken Symmetry and Correlation Functions*, 2nd ed. (W.A. Benjamin, Inc. ,Reading Mass., 1975) P.74

[4] P. 254 of ref. 2

[5] D.R. Nelson and J.M. Kosterlitz, Phys. Rev. Lett. **39**, 1201 (1977).

[6] N. Bogoliubov, J. Phys. USSR, **11**, 23 (1947)

[7] K. Huang and C.N. Yang, Phys. Rev. **106**, 1135 (1957).

[8] A. Abrikosov, L. Gorkov and I. Dzyaloshinski, *Methods of Quantum Field Theory in Statistical Physics* (1970) ; A.L. Fetter and J.D. Walecka, *Quantum Theory of Many Particle System* (1971) ; K. Huang, *Statistical Mechanics*, (John Wiley & Sons, Inc. 1987)

[9] Landau and Lifshitz, *Statistical Physics*, part 2, P.88, (Pergamon Press Ltd. 1980)

[10] J. Kosterlitz and D. Thouless, J. Phys. C **6**, 1181 (1973) ; J. Kosterlitz, J. Phys. C **7**, 1046 (1974)

[11] J. Ziman, *Models of Disorder*, (Cambridge University Press, 1979)

[12] M.H.W. Chan, K.I. Blum, S.Q. Murphy, G.K.S. Wong, and J.D. Reppy, Phys. Rev. Lett. **61**, 1950 (1988) ; G.K.S. Wong, P.A. Crowell, H.A. Cho, and J.D. Reppy, Phys. Rev. Lett., **65**, 2410 (1990).

[13] For a comprehensive review see J.D. Reppy, J. Low Temp. Phys., **87**, 205 (1992).

[14] A. Khurana, Physics Today, July 1989, P.17

[15] R. Vacher, T. Woignier and Pelous , Phys. Rev. B **37**, 6500 (1988).

Chapter Two

Hard-Sphere Bos Gas in Random External Potentials *

2.1 Abstract

We consider a dilute hard-sphere Bose gas in random external potentials at low temperatures, in D=3, using the technique of pseudopotentials and the Bogoliubov transformation. At absolute zero, the random potentials can deplete the Bose condensate, though not completely. On the other hand, they generate an amount of normal fluid equal to 4/3 the condensate depletion. This is a localization effect that can destroy superfluidity at absolute zero. General features of the superfluid density in the neighborhood of this transition point agree qualitatively with experimental results on helium in porous media.

2.2 Introduction

We report on some results concerning the low-temperature properties of a dilute hard-sphere Bose gas in random external potentials in 3 dimensions. Such a model is a crude simulation of superfluid helium in porous media [1]. The sponge-like media are here idealized as random distributions of hard-sphere potentials. To make the problem tractable, we further assume that the randomness is sufficiently dilute, and the temperature sufficiently low, that the hard-spheres can be approximated by delta-function pseudopotentials [2]. We also assume that the potentials are distributed with uncorrelated randomness. Thus, the very large pores that are apparently present in the experimental media are not taken into account here. The purpose of this study is not to construct a quantitative model for the experiments, but to illuminate some qualitative features. We are able to show, for example, that at absolute zero superfluidity can be destroyed by the randomness, through an effect suggestive of boson localization.

From a theoretical point of view, the interparticle interactions are necessary, to prevent a total condensation into a single localized orbital in the external potential. Thus, unlike the much-studied case of fermions, one does not have the luxury of treating the potentials as perturbations on a free-particle Hamiltonian. Here we do the next best thing, namely, start with the simplest soluble problem involving interparticle interactions — a dilute hard-sphere gas at low temperatures[2,3]. This approach differs from previous efforts on this subject[4,5], in that ours is a microscopic low-density low-temperature model, rather than a phenomenological "tight-binding" model. It may illuminate the problem from a different angle.

27

2.3 Hamiltonian and Its Diagonization

We consider a grand ensemble with chemical potential μ, with Hamiltonian H given by (with $\hbar = 1$)

$$H - \mu N = \int d^3 x \; \psi^\dagger \left(-\frac{1}{2m} \nabla^2 - \mu + U \right) \psi + \frac{1}{2} v_0 \int d^3 x \; \psi^\dagger \psi^\dagger \psi \psi \qquad (1)$$

where $\psi(x)$ is the field operator for non-relativistic boson of mass m, $N = \int d^3 x \; \psi^\dagger \psi$ is the number operator, $U(x)$ is the external potential, and $v_0 = 4\pi a/m$, where a is the hard sphere diameter. The ground state energy is rendered finite by subtracting an appropriate divergent constant[3].

The external potential $U(x)$ may be pictured as a sum of of randomly located scattering centers of random strengths, either attractive or repulsive. We assume $\langle U(x)U(y) \rangle_{av} \propto \delta^3(x - y)$, and characterize the potentials by a single parameter R_0:

$$\frac{1}{V} \langle |U_k|^2 \rangle_{av} = R_0 \qquad (2)$$

where V is the total volume of the system, U_k is the Fourier transform of $U(x)$, and the subscript av denotes a quenched average over potentials. It has dimension (energy)^2 (length)^3, and is (average density)$\times$(mean-square strength) of the individual scatterers, the strength being measured by the spatial integral of the potential. Keeping R_0 fixed while varying the density of the bosons is like varying the coverage of the liquid helium in a porous medium.

Proceeding in a standard fashion[3], we introduce free-particle annihilation and creation operators a_k and $a_k^\dagger$, and assume the single level with $k = 0$ is macroscopically occupied, with occupation number N_0. We refer to $n_0 = N_0/V$ as the condensate density. In the

expansion of H in terms of a_k and $a_k^\dagger$, we neglect all off-diagonal terms except those of the form $v_0 a_0^\dagger a_0^\dagger a_k a_k$ and $U_k a_0^\dagger a_k$, and their hermitian conjugates. We then replace all occurrences of a_0 and $a_0^\dagger$ by the c-number $\sqrt{N_0}$. Thus, the only processes considered are the annihilation of a pair $\{k, -k\}$ into the condensate through the hard-sphere interaction, and the scattering of a single particle k into the condensate by the random potentials, and the corresponding inverse processes. The effective Hamiltonian is

$$
\begin{aligned}
H_{eff} - \mu N = \; & V(-\mu n_0 + \frac{1}{2} v_0 n_0^2) + \sum_{k \neq 0} (\frac{k^2}{2m} - \mu + 2 v_0 n_0) a_k^\dagger a_k \\
& + \left(\frac{n_0}{V}\right)^{1/2} \sum_{k \neq 0} (U_k a_k^\dagger + U_{-k} a_k) + \frac{1}{2} v_0 n_0 \sum_{k \neq 0} (a_k a_{-k} + a_k^\dagger a_{-k}^\dagger) \\
& + \frac{v_0}{V} \left[\sum_{k \neq 0} a_k^\dagger a_k\right]^2
\end{aligned}
\tag{3}
$$

The last term is important when the condensate becomes depleted. We treat it in a mean-field fashion by making the replacement

$$
\frac{1}{V} \left[\sum_{k \neq 0} a_k^\dagger a_k\right]^2 \rightarrow n' \sum_{k \neq 0} a_k^\dagger a_k
\tag{4}
$$

where n' is a parameter to be determined later. The small parameters in our perturbation theory are a and R_0.

The effective Hamiltonian is diagonalized by a Bogoliubov transformation:

$$
a_k = \frac{c_k - \alpha_k c_{-k}^\dagger}{\sqrt{1 - \alpha_k^2}} - \frac{1}{\omega_k} \left(\frac{n_0 U_k}{V} \frac{1 - \alpha_k}{1 + \alpha_k}\right)^{1/2}
\tag{5}
$$

where

$$
\begin{aligned}
\alpha_k &= 1 + x - \sqrt{x(x+2)}, \quad \omega_k = v_0 n_0 \sqrt{x(x+2)} \\
x &= \frac{k^2}{2 m n_0 v_0} + \Delta, \qquad\qquad \Delta = \frac{v_0(n_0 + n') - \mu}{v_0 n_0}
\end{aligned}
\tag{6}
$$

29

We set $\Delta = 0$, to insure that the quasi-particle spectrum ω_k has no energy gap, in conformity with general theorems[6]. This condition determines n'. The diagonalized quench-averaged Hamiltonian has the form

$$H_{eff} - \mu N = V(-\mu n_0 + \epsilon_0) + \sum_{k \neq 0} \omega_k c_k^\dagger c_k$$

$$\epsilon_0 = \frac{2\pi a n_0^2}{m} \left[1 + \frac{128}{15\sqrt{\pi}}(n_0 a^3)^{1/2} \right] + \frac{2 - \sqrt{2}}{\sqrt{\pi}} m n_0^{3/2} a^{1/2} R_0 \tag{7}$$

The first term recovers well-known results[3].

The grand partition function $Q = \text{Tr} \exp[-\beta(H - \mu N)]$ is a sum over N_0, but we keep only the largest term. Thus, μ and N_0 are determined by the two conditions[7]

$$\frac{\partial}{\partial n_0} \frac{\ln Q}{V} = 0,$$

$$n = n_0 + \frac{1}{V} \sum_{k \neq 0} \langle a_k^\dagger a_k \rangle \tag{8}$$

where n is the particle density. and $\langle \rangle$ denotes grand ensemble average. ¿From these conditions we can obtain n' and n_0 as functions of n and the temperature.

The average number of particles with nonzero momentum represents a depletion of the condensate:

$$\frac{1}{V} \sum_{k \neq 0} \langle a_k^\dagger a_k \rangle = n_1 + n_R$$

$$n_1 = \frac{8\sqrt{\pi}}{3}(n_0 a)^{3/2} + \frac{4}{\sqrt{\pi}\lambda^3} \int_0^\infty dt \frac{t^2(t + \theta/2)}{\sqrt{t^2 + \theta}\{\exp[t\sqrt{t^2 + \theta}] - 1\}} \tag{9}$$

$$n_R = \frac{m^2}{8\pi^{3/2}} \left(\frac{n_0}{a} \right)^{1/2} R_0$$

$$\lambda = \sqrt{2\pi\beta/m}, \quad \theta = 2\beta v_0 n_0$$

where n_1 arises from the hard-sphere interactions[3,7]. It is very small at absolute zero, and rises quadratically with increasing temperature. The term n_R corresponds to condensate

depletion due to scattering of condensate particles with the random potentials. The fractional depletion is of the order of $m^2 R_0/\sqrt{na}$. The factor $1/\sqrt{a}$ underscores the fact that the system would collapse if there were no interparticle interactions. The depletion can be substantial within the validity of our approximations. On the other hand, there cannot be total depletion, for $n_0 = 0$ is not a possible solution at absolute zero, for any finite R_0. (See below.)

2.3 Superfluid Density at Low Temperatures

The superfluid density n_s is obtained by considering the response of the momentum density to an externally imposed velocity field[8,9]. The relevant response function is

$$R^{ij}(x,t) = \langle[g^i(x,t),g^j(0,0)]\rangle = \int \frac{d^3k\ d\omega}{(2\pi)^4} e^{i(k\cdot x-\omega t)} R^{ij}(k,\omega)$$

$$g^j(x,t) = (2i)^{-1}\psi^\dagger(x,t)\overleftrightarrow{\partial^j}\psi(x,t)$$

(10)

where $\psi(x,t)$ is a Heisenberg operator. The static susceptibility is given by

$$\chi^{ij}(k) = \int_{-\infty}^{\infty} \frac{d\omega}{2\pi} \frac{R^{ij}(k,\omega)}{\omega - i\epsilon} \equiv \frac{k^i k^j}{k^2} A(k^2) + \left(\delta_{ij} - \frac{k^i k^j}{k^2}\right) B(k^2)$$

(11)

The transverse susceptibility $B(0)$ is the normal fluid mass density. The superfluid mass density is accordingly $\rho_s = \rho - B(0)$, where ρ is the total mass density.

Using particle conservation, one can show that $A(0) = \rho$, which is a form of the f-sum-rule. Thus one sometimes writes $\rho_s = A(0) - B(0)$. However, this is not valid for the present calculation, because particle conservation was violated in replacing a_0 by a c-number. We have in effect truncated the Hilbert space, leaving out the subspace spanned by single-particle states of zero momentum. Thus, computations involving the time evolution of zero-momentum particle-states would be falsified. On the other hand,

31

the nonzero momentum sector should be unaffected, (as long as second-order effects of the zero-momentum states are unimportant.) In the present context, this means that we can trust a calculation of $B(0)$ but not $A(0)$. Accordingly, we calculate the superfluid density through $\rho - B(0)$, and not $A(0) - B(0)$[10].

The calculation of $B(0)$ is quite tedious. The details can be found in the appendix. The superfluid density $n_s = \rho_s/m$ is found to be

$$
\begin{aligned}
n_s &= n - n_2 - \frac{4}{3}n_R \\
n_2 &= -\frac{1}{3m} \int \frac{d^3p}{(2\pi)^3} p^2 \frac{\partial n_p}{\partial \omega_p} = \frac{8}{3\sqrt{\pi}\lambda^3} \int_0^\infty dt \frac{t^4 \exp[-t\sqrt{t^2 + \theta}]}{\left\{1 - \exp[-t\sqrt{t^2 + \theta}]\right\}^2}
\end{aligned}
\tag{12}
$$

where $n_p = [\exp(\beta\omega_p) - 1]^{-1}$ is the average number of phonons. There is an elementary derivation of n_2 based on Gallilean invariance in the absence of random potentials[11]; but we know of no intuitive way to obtain the term $4n_R/3$. The factor 4/3 indicates that the random potentials generate more normal fluid than they took from the condensate. This makes it possible to destroy superfluidity at absolute zero. To see this, note that from $n_R = n - n_0 - n_1$ and $n_s = n - \frac{4}{3}n_R$, we have

$$
n_s = \frac{1}{3}[4(n_0 + n_1) - n]
\tag{13}
$$

which vanishes when the condensate is roughly 3/4 depleted by the random potentials. This result means that part of the condensate, which is made up of zero-momentum particles, belongs to the normal fluid, i.e., they are dragged along by the random potentials. This indicates localization, or formation of bound states of macroscopic extensions.

We can obtain n_0 at low temperatures ($T \rightarrow 0$) from (8) by iteration. Using this result, we then calculate n_s as a function of n and T. Neglecting a term of order $\sqrt{na^3}$ for

32

simplicity, we have

$$\frac{n_0}{n} \approx e^{-2\phi} - \frac{1}{\cosh\phi}\left(\frac{T}{T_1}\right)^2 + \frac{K_1(\phi)}{\sqrt{na^3}}\left(\frac{T}{T_1}\right)^4$$

$$\frac{n_s}{n} \approx \frac{1}{3}\left(4e^{-2\phi} - 1\right) + \frac{4}{3}e^\phi \tanh\phi\left(\frac{T}{T_1}\right)^2 - \frac{K_2(\phi)}{\sqrt{na^3}}\left(\frac{T}{T_1}\right)^4 \tag{14}$$

where

$$\sinh\phi = \frac{m^2 R_0}{16\pi^{3/2}\sqrt{na}}$$

$$T_1 = \sqrt{3/2}\pi^{-5/4}m^{-1}n^{3/4}a^{1/4}$$

$$K_1(\phi) = \frac{3}{1280}\frac{e^{4\phi}}{\sqrt{2\pi}} \tag{15}$$

$$K_2(\phi) = \frac{e^{5\phi}}{16\pi^{9/2}}\left(1 + \frac{\pi^4}{20\sqrt{2}}\tanh\phi\right)$$

At $T = 0$, n_0 never vanishes. On the other hand, $n_s = 0$ at $\phi = \ln 4/2$, which corresponds to a critical density n_c given by $n_c a^3 = (m^2 a R_0)^2/36\pi^3$. This value lies within the regions of validity of our approximation.

Fig.2.1 shows a 3D plot of n_s as given by (14), for certain values of a and R_0. The surface has a nose shape, which describes a kind of "reentrant" behavior. Generally, n_s rises quadratically with T, goes through a maximum, and then vanishes linearly at a critical temperature, which is roughly given by $T_c \propto an/m$, except near the tip of the "nose". The critical index is thus the same as that for the ideal Bose gas. This is in agreement with experimental results on liquid helium in porous media. But the non-monotonic behavior of n_s has not been detected so far.

It may seem curious that n_s initially increases with T. We have to remember, however, that n_s is strongly suppress by the random potentials at $T = 0$. As T starts to increase, the suppression is lessened, because less normal fluid is generated by the random potentials, due to the fact that n_0 decreases.
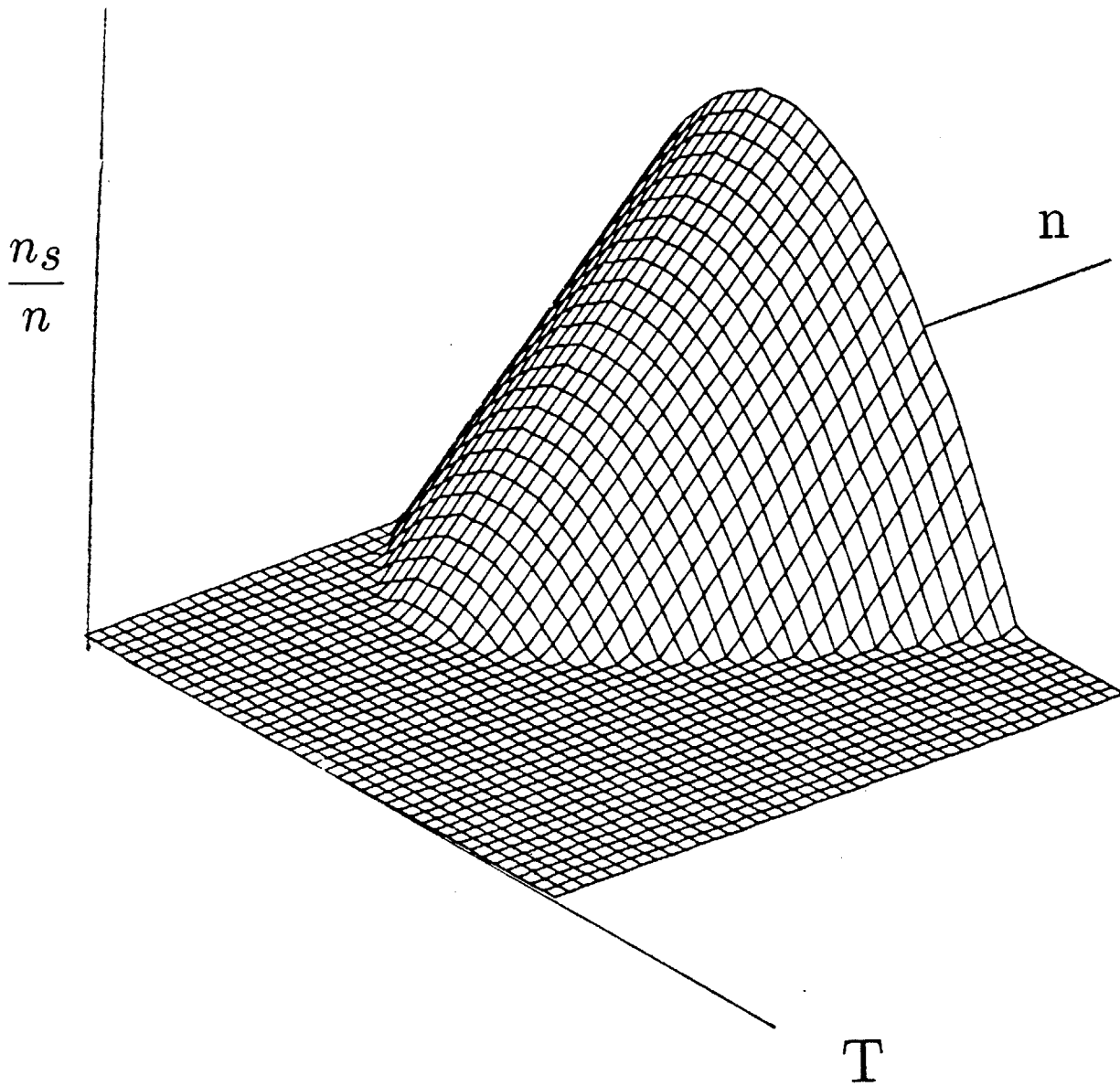
Fig. 2.1

Superfluid density as function of temperature and density, in the neighborhood of the superfluid transition point at absolute zero.

Going back to (8), we can study the thermodynamic behavior near $n_0 = 0$, i.e., the Bose-Einstein transition point of the ideal gas. In this region our model is similar to a soluble one[12], in which ω_k is replaced by $k^2/2m$. The isotherms are of the van der Waals type, exhibiting first-order phase transitions, with a very narrow transition region, of order $\sqrt{na^3}$. The presence of random potentials does not change the qualitative behavior. Because scattering between quasi-particles has been neglect, however, the model cannot be taken seriously in this domain.

In regard to low-temperature phase transitions, our theory is of the mean-field type, because all fluctuations in the condensate have been ignored. In this approximation, the condensate cannot react to the destruction of superfluidity. For this reason, no specific heat singularities appear at the transition point, and the condensate remains structureless in the region $n < n_c$, the so-called "Bose glass" phase. These inadequacies can be remedied only by improving on the Bogoliubov transformation, which we are attempting to do.

Appendix: Calculation of Normal Fluid Part

By definition

$$R^{ij}(x,t) = \frac{1}{2} < [g^i(x,t), g^j(0,0)] > = \int \frac{dk^3 d\omega}{(2\pi)^4} e^{i(k \cdot x - \omega t)} R^{ij}(k,\omega) \qquad (A1)$$

We write down the expression for $R^{ij}(x,t)$ first then calculate $R^{ij}(k,\omega)$ using the inverse Fourier transform :

$$R^{ij}(k,\omega) = \int d^3x \, dt \, e^{-i(k \cdot x + \omega t)} R^{ij}(x,t)$$

Expand the momentum density oprator in terms of a's and $a^\dagger$'s, we got

$$g^{ij}(x,t) = \frac{1}{2V} \sum_{p,q} e^{-i(p-q) \cdot x} (p+q)^i a_p^\dagger(t) a_q(t) \qquad (A2)$$

So if we define

$$I^{ij}(x,t) = < [g^i(x,t), g^j(0,0)] >$$

$$= \frac{1}{4V^2} \sum_{\substack{p,q \\ p',q'}} e^{-i(p-q) \cdot x} (p+q)^i (p'+q')^j < [a_p^\dagger(t) a_q(t), a_{p'}^\dagger a_{q'}] > \qquad (A3)$$

$R^{ij}(k,\omega)$ can be easily obtained from I by

$$R^{ij}(k,\omega) = \int d^3x \, dt \, e^{-i(k \cdot x - \omega t)} \frac{1}{2} I^{ij}(x,t)$$

Furthermore , the liner response function χ^{ij} can be calculated by

$$\chi^{ij}(k) = \frac{1}{\pi} \int_{-\infty}^{\infty} \frac{d\omega}{w - i\epsilon} R^{ij}(k,\omega) \qquad (A4)$$

36

There is an $i\epsilon$ in the denumerator because we assume the external potential is propotional to $e^{\epsilon t}$. It means the external potential is turned on adiabaticaly from $t = -\infty$ to $t = 0$.

Define another quantity $W_{pq,p'q'} =< [a_p^\dagger(t)a_q(t), a_{p'}^\dagger, a_{q'}] >$ which is the ensemble average in $(A3)$.

Because the hamiltonian is diagonized by a Bogoliubov transformation. We can find out the time dependence of all operators. It's easy to see ,and will be calculated explicitly later, that all the commutators invloved in the expansion of W defined above are c-numbers , so we can factor them out of the ensemble average $< \cdots >$.

We got

$$W_{pq,p'q'} =< a_p^\dagger(t)a_{q'} > [a_q(t), a_{p'}^\dagger]+ < a_p^\dagger(t)a_{p'}^\dagger > [a_q(t), a_{q'}]$$

$$+ < a_p^\dagger(t)a_{q'} > [a_q(t), a_{p'}^\dagger]+ < a_{p'}^\dagger a_q(t) > [a^\dagger(t), a_{q'}] \qquad (A5)$$

From (7), we know $c_k(t) = e^{-i\omega_k t}c_k$ and use the relation (5) we can calculate W at anytime t.

Substitute everthing in we get the expresion

$$W_{pq,p'q'} = \delta(p - q')\delta(q - p')(y_p V_q - y_q^* V_p^*)$$

$$+\delta(p + p')\delta(q + q')(x_p T_q + x_q^* T_p) \qquad (A6)$$

where $T_p = u_p v_p(e^{i\omega_p t} - e^{-i\omega_p t})$ and $V_p = u_p^2 e^{-i\omega_p t} - v_p^2 e^{i\omega_p t}$ for $p > 0$ zero for $p = 0$.

And

$$x_p = -u_p v_p \left[n_p e^{i\omega_p t} + (1 + n_p)e^{-i\omega_p t} \right] + h_p$$

$$y_p = u_p^2 n_p e^{i\omega_p t} + v_p^2(1 + n_p)e^{-i\omega_p t} + h_p$$

Finally, u, v, n and h are defined as follows:

$$u_p = \frac{1}{\sqrt{1 - \alpha_p^2}}, \; v_p = \frac{\alpha}{\sqrt{1 - \alpha_p^2}}, \; n_p = <c_p^\dagger c_p> = \frac{1}{e^{\beta \omega_p} - 1}$$

$$h_p = \frac{|U_p|^2}{V n_0 v_0^2 (1 + z_p)^2}, \; z_p = x_p + 1$$

If we substitue $(A6)$ into $(A3)$, we got $I^{ij}(k,t)$ equal to

$$\frac{1}{4V} \sum_p \left[(2p + k)^i(2p + k)^j \left(y_p V_{p+k} - x_p T_{p+k} \right) - (2p - k)^i(2p - k)^j \left(y_p^* V_{p-k}^* + x_p^* T_{p-k} \right) \right]$$

$$(A7)$$

Saperate the summation to $p = 0$ and $p > 0$ parts. We can write

$$I^{ij} = I_0^{ij} + I_1^{ij}$$

where

$$I_0^{ij} = \frac{N_0}{4V} k^i k^j [(V_k - V_{-k}^*) - (T_k + T_{-k})]$$

$$= -\frac{N_0}{4V} k^i k^j \left(\frac{1 + \alpha_k}{1 - \alpha_k} \right) \left(e^{i\omega_k t} - e^{-i\omega_k t} \right)$$

I_1^{ij} is the same as I^{ij} except $\sum_p$ is replced by $\sum_{p>0}$.

Similarly, we break $R^{ij}(k, \omega)$, $\chi^{ij}(k)$, A and B in (13) into two parts also. Denote them by subscript 0 and 1.

38

If we substitue everything in , we will find

$$R_0^{ij}(k,\omega) = -\frac{1}{2}\frac{N_0}{4V}k^i k^j \left(\frac{1+\alpha_k}{1-\alpha_k}\right) 2\pi[\delta(\omega+\omega_k) - \delta(\omega-\omega_k)]$$

$$\chi_0^{ij}(k) = \frac{1}{\pi}\int_{-\infty}^{\infty}\frac{d\omega}{\omega-i\epsilon}R_0^{ij}(k,\omega)$$

$$= \frac{N_0}{2V}k^i k^j \left(\frac{1+\alpha_k}{1-\alpha_k}\right)\frac{1}{\omega_k} = \left(\frac{mN_0}{V}\right)\frac{k^i k^j}{k^2}$$

So we find

$$A_0(k^2) = \frac{mN_0}{V}\,,\ B_0(k^2) = 0 \tag{A8}$$

Now consider I_1^{ij} and χ_1^{ij}. From $(A7)$, we can write χ_1^{ij} in the form

$$\chi_1^{ij}(k) = \frac{1}{2\pi}\int_{-\infty}^{\infty}\frac{d\omega}{\omega-i\epsilon}\int_{-\infty}^{\infty}e^{i\omega t}I_1^{ij}(k,t)\,dt$$

$$= \frac{1}{4V}\sum_{p>0}\left[(2p+k)^i(2p+k)^j f_1(p,k) - (2p-k)^i(2p-k)^j f_2(p,k)\right] \tag{A9}$$

After tedious but straight forward calculation , we find

$$f_1(p,k) = \frac{1}{\omega_{p+k}+\omega_p}\left[u_{p+k}^2 v_p^2 - u_p u_{p+k} v_p v_{p+k} + n_p(u_p v_{p+k} - u_{p+k} v_p)^2\right]$$

$$+\frac{1}{\omega_{p+k}-\omega_p}\left[v_p^2 v_{p+k}^2 - u_p u_{p+k} v_p v_{p+k} + n_p\left(u_p u_{p+k} - v_p v_{p+k}\right)^2\right]$$

$$+\frac{h_p}{\omega_{p+k}}\left(u_{p+k} + v_{p+k}\right)^2 \tag{A10}$$

Call the first line f_{11} the second line f_{12} and the third f_{13} for later convenience.

A It turns out that $f_2(p,k) = f_1(-p,k)$. If we make the change of variable $p \mapsto -p$ in the second term in the summation in (A9), we will find

39

$$\chi_1^{ij} = \frac{1}{2V} \sum_{p>0} (2p+k)^i (2p+k)^j f_1(p,k) \qquad (A11)$$

Because there turns out to be no ambiguity coming from the $i\epsilon$ in the denumerator, we negnect them in the following calculations. It's easy to see $f_{11} \mapsto 0$ as $k \mapsto 0$. So we can neglect it since eventually we have to take that limit. Substitute $(A10)$ into $(A11)$, we have

$$\chi_1^{ij}(k) = \chi_{11}^{ij}(k) + \chi_{12}^{ij}(k) + \chi_{13}^{ij}(k)$$

where

$$\chi_{11}^{ij}(k) = \frac{1}{2V} \sum_{p>0} (2p+k)^i (2p+k)^j \frac{h_p}{\omega_{p+k}} (u_{p+k} + v_{p+k})^2$$

$$\chi_{12}^{ij}(k) = \frac{1}{2V} \sum_{p>0} \frac{(2p+k)^i (2p+k)^j}{\omega_{p+k} - \omega_p} \left[v_p^2 v_{p+k}^2 - u_p u_{p+k} v_p v_{p+k} \right]$$

$$\chi_{13}^{ij}(k) = \frac{1}{2V} \sum_{p>0} \frac{(2p+k)^i (2p+k)^j}{\omega_{p+k} - \omega_p} n_p (u_p u_{p+k} - v_p v_{p+k})^2$$

If we make a change of variable $p \mapsto -p - k$ in χ_{12}^{ij} , the integrand flips sign. It means χ_{12}^{ij} is exactly zero.

In the same way χ_{13}^{ij} is equal to

$$\frac{1}{4V} \sum_{p>0} (2p+k)^i (2p+k)^j \frac{n_p - n_{p+k}}{\omega_{p+k} - \omega_p} (u_p u_{p+k} - v_p v_{p+k})^2 \qquad (A12)$$

It's now the right time to take the limit $k \mapsto 0$. First

$$\lim_{k \mapsto 0} \chi_{11}^{ij}(k) = \frac{1}{2V} \sum_{p>0} 4p^i p^j (u_p + v_p)^2 \frac{h_p}{\omega_p}$$

40

$$= \delta^{ij} \frac{2}{3V} \sum_{p>0} p^2 \frac{2m}{p^2} h_p = \frac{4}{3} \frac{m}{V} \sum_p h_p$$

$$= \frac{4}{3} m n_R \delta^{ij}$$

So we have

$$A_{11}(0) = B_{11}(0) = \frac{4}{3} n_R \qquad (A13)$$

Next we consider χ_{13}^{ij}:

$$\lim_{k \mapsto 0} \chi_{13}^{ij}(k) = \frac{1}{4V} \sum_{p>0} \left[\lim_{k \mapsto 0} (2p+k)^i (2p+k)^j (u_p u_{p+k} - v_p v_{p+k}) \frac{n_p - n_{p+k}}{\omega_{p+k} - \omega_p} \right]$$

$$= \delta^{ij} \frac{1}{4V} \frac{4}{3} \sum_{p>0} p^2 \left(-\frac{\partial n(\omega)}{\partial \omega} \right)$$

$$= -\delta^{ij} \frac{1}{3} \int_{-\infty}^{\infty} \frac{d^3 p}{(2\pi)^3} p^2 \frac{\partial n(\omega)}{\partial \omega} \qquad (A14)$$

Note that $n(x) = \frac{1}{e^x - 1}$, $n'(x) = \frac{dn(x)}{dx}$.

Because of the δ^{ij} in front of the whole expression, we have

$$A_{13}(0) = B_{13}(0) = -\frac{1}{3} \beta \int \frac{d^3 p}{(2\pi)^3} p^2 n'(\omega_p)$$

$B_{13}(0)$ is nothing but the normal fluid density derived using Galelian invarience thirty years ago.[1]

For the conveniece of low temperatire expansion , we cast $B_{13}(0)$ into the followinf form:

$$B_{13}(0) = -\frac{1}{3} \frac{1}{2\pi^2} \int_0^{\infty} p^4 \frac{\partial n}{\partial p} \frac{\partial p}{\partial \omega} dp$$

$$= \frac{1}{3} \frac{1}{2\pi^2} \int_0^{\infty} n_p \frac{\partial}{\partial p} \left(p^4 \frac{\partial p}{\partial \omega} \right) dp$$

41

$$= \frac{1}{3} \frac{m}{\pi^2} \int_0^\infty p^3 \frac{6p^4 + 9\lambda p^2 + 4\lambda^2}{(2p^2 + \lambda)^2 \sqrt{p^2 + \lambda}} n_p \, dp \qquad (A15)$$

where $\lambda = 4mn_0v_0$. For the ideal gas case, $\lambda \mapsto 0$. So $B_{13}(0) \mapsto \frac{m}{2\pi^2} \int_0^\infty p^2 n_p \, dp$ which

is exactly the density of particles not in the condensate for free particles.

References

1. M.H.W. Chan, K.I. Blum, S.Q. Murphy, G.K.S. Wong, and J.D. Reppy, Phys. Rev. Lett. **61**, 1950 (1988); G.K.S. Wong, P.A. Crowell, H.A. Cho, and J.D. Reppy, Phys. Rev. Lett. **65**, 2410 (1990).

2. K. Huang and C.N. Yang, Phys. Rev. **105**, 767 (1957).

3. T.D. Lee, K. Huang, and C.N. Yang, Phys. Rev. **106**, 1135 (1957).

4. P.B. Weichman, M. Rasolt, M.E. Fisher, and M.J. Stephen, Phys. Rev. **B33**, 4632 (1986).

5. M.P.A. Fisher, P.B. Weichman, G. Grinstein, and D.S. Fisher, Phys. Rev. **B40**, 546 (1989).

6. N.M. Hugenholtz and D. Pines, Phys. Rev. **116**, 489 (1959).

7. A.E. Glassgold, A.N. Kaufman, and K.M. Watson, Phys. Rev. **120**, 660 (1960).

8. P.C. Hohenberg and P.C. Martin, Ann. Phys. **34**, 291 (1965).

9. D. Forster, *Hydrodynamic Fluctuations, Broken Symmetry, and Correlations Functions*, (W.A. Benjamin, Reading, MA, 1975), p.221.

10. Explicit calculation in this model gives $A(0) - B(0) = mN_0$, the ideal-gas value.

11. I.M. Khalatnikov, *Introduction to the Theory of Superfluidity*, (W.A. Benjamin, New York, 1965), p.13.

12. K. Huang, C.N. Yang, and J.M. Luttinger, Phys. Rev. **105**, 776 (1957).

Chapter Three

Two Dimensional Interacting Boson System

3.1 How 2D System Differs From a 3D One

In this chpater we expand the microscopic Hamiltonian of self-interacting boson system in terms of the density and phase operators which are canonical conjugates to each other. When terms higher than the second order are neglected, the Hamiltonian can be diagonized in a fashion just like the harmonic oscillators. This method is applied to two physical systems: superfluid helium and fractional quantum Hall effect (FQHE). We shall first derive the expression of superfluid density for 2D system where canonical treatment has been lacking. We then reproduce the 3D results obtained by the Bogoliubov transformation. Finally, we shall show that the basic phenomenologies of fractional quantum Hall effect at exact filling numbers can be derived without the introduction of the Chern-Simons term [1].

The microscopic model for the low temperature properties of the three dimensional self-interacting boson system has been well established [2]. However, unlike the corresponding 3D system no similar microscopic quantum theory for 2D system has been achieved. In 3D system there is a bose condensate caused by the spontaneous symmetry breaking when the temperature is low enough. Thus we can diagonize the microscopic Hamiltonian by expanding the field operator around its mean value and keep the deviation up to the second order. The meaning of this procedure is that at low temperature only the immediate

neighborhood of some particular vacuum contributes to the statistical ensemble. All the other vacua related by global gauge transformations are not accessible by thermal flutuations. In 2D case the above argument does not go through because bose condensate dose not exist at any finite temperature. In other words, the mean value of the field operator is zero and all the vacua have to be taken into account.

In order to obtain the low energy eigenstates, we propose a new way to diagonize the Hamiltonian by expanding the density, instead of the field, operator around its mean value which is always finite. This method is valid for an arbitrary dimension as long as the density fluctuation is small. The existence of the condensate is not required. External potential can be easily included in this scheme since it is linearly coupled to the density operator.

As a model for the superfluid helium, we are interested in how the superfluid density ρ_s depends on the temperature and the strength of the external random potential, if present. We will derive the explicit formula of ρ_s for both 2D and 3D cases. Another important quantity is the condensate density n_0, which is the square of the expectation value of the field operator. n_0 is nonzero as long as there is a spontaneous symmetry breaking. As mentioned above, in 2D system phase fluctuation is so strong that n_0 vanishes in arbitrary finite temperature. Within the present model we are able to see how the condensate disappears when we reduce the thickness of a 3D slab. This also provides a criterion to determine when we can treat the slab as a 3D system and when a 2D one.

In addition to superfluid helium, it turns out that our method has a direct application to the problem of fractional quantum Hall effect [3]. We follow the work of Zhang, Hansson

and Kivelson [1] to map the 2D fermion problem to a 2D equivelant boson problem. It will be shown that the boson Hamiltonian can be diagonized in a rather similar fashion as the superfluid without introducing the auxilary Chern-Simons term[1]. The spectrum of the elementary excitation and the Hall conductivity will be calculated. Both of them agree with the well-known results.

3.2 Low Energy Eigenstates

The Hamiltonian H in terms of the quantum field operator Ψ is

$$
H = \int \frac{1}{2m} \vec{\nabla} \Psi^\dagger(x) \vec{\nabla} \Psi(x) d^d x - \mu \int \Psi^\dagger(x) \Psi(x) d^d x
$$
$$
+ \frac{1}{2} \int \Psi^\dagger(x) \Psi^\dagger(y) v(x - y) \Psi(x) \Psi(y) d^d x d^d y \tag{1}
$$

Instead of $\Psi(x)$ and $\Psi^\dagger(x)$, we choose hermitean operators ρ and Φ as the basic operators

$$
\Psi(x) = \sqrt{\rho(x)} e^{i\Phi(x)} , \quad \Psi^\dagger(x) = e^{-i\Phi(x)} \sqrt{\rho(x)} \tag{2}
$$

If we impose the commutation relation between Φ and ρ such that the original commutation relation $[\Psi(r), \Psi^\dagger(r')] = \delta(r - r')$ is reproduced, then we get an equivalent Hamiltonian in terms of Φ and ρ with exactly the same spectrum. It turns out that the correct choice is

$$
[\Phi(r), \rho(r')] = -i\delta(r - r') \tag{3}
$$

This means that the "phase" operator Φ is the canonical conjugate of the "density" operator ρ. Assuming that the fluctuation of $\rho(x)$ around its mean value ρ_0 is small, we expand $\sqrt{\rho(x)}$ in the form

$$
\sqrt{\rho(x)} = [\rho_0 + \eta(x)]^{\frac{1}{2}} \simeq \sqrt{\rho_0}(1 + \frac{\eta}{2\rho_0})
$$

46

Let n be the particle density, we have $n = <\rho> \simeq \rho_o$. Substituting this into H, we get

$$H \simeq \frac{1}{2m} \int \left[\frac{1}{4\rho_0}(\vec{\nabla}\eta)^2 + \rho_0(\vec{\nabla}\Phi)^2 \right] d^d x - \mu \int \eta d^d x$$
$$+ v_0\rho_0 \int \eta d^d x + \frac{v_0}{2} \int \eta^2 d^d x$$

where $v_0 = \int v(x) d^d x$. An infinite constant is neglected. Choosing ρ_0 such that terms linear in η vanish, we have

$$\rho_0 = \frac{\mu}{v_0}$$

Now we can write the Hamiltonian in the simple form

$$H = \frac{1}{2m} \int \left[\frac{1}{4\rho_0}(\vec{\nabla}\eta)^2 + \rho_0(\vec{\nabla}\Phi)^2 + \lambda\eta^2 \right] d^d x \qquad (4)$$

where $\lambda = mv_0$. It's clear now that this Hamiltonian can be diagonized in the momentum representation. Let

$$\eta(r) = \frac{1}{\sqrt{V}} \sum_k e^{ikr} q_k \ , \quad \Phi(r) = \frac{1}{\sqrt{V}} \sum_k e^{ikr} p_{-k}$$

Since η, Φ are hermitean we have the relations $q_k = q_{-k}^\dagger$, $p_k = p_{-k}^\dagger$. They satisfy the commutation relation

$$[p_k, q_{k'}] = -i\delta_{k,k'}$$

In terms of p_k and q_k, H becomes

$$H = \frac{1}{2m} \sum_k \left(\frac{k^2}{4\rho_0 + \lambda} \right) q_k q_{-k} + \rho_0 k^2 p_k p_{-k} \qquad (5)$$

Let's further define

$$a_k \equiv \sqrt{\frac{\alpha_k}{2}} (q_k - \frac{i}{\alpha_k} p_{-k})$$

47

and express p_k, q_k in terms of a_k :

$$q_k = \frac{1}{\sqrt{2\alpha_k}}(a_k + a^\dagger_{-k})$$

$$p_k = \frac{-i\alpha_k}{\sqrt{2\alpha_k}}(a_k - a^\dagger_{-k})$$

(6)

The commutation relation between a_k and $a^\dagger_k$ is

$$[a_k, a^\dagger_{k'}] = \delta_{k,k'}$$

Substitute eq.(6) into H and choose α_k such that the off-diagonal terms in H vanishes.

We get

$$\alpha_k = \left[\frac{1}{\rho_0 k^2}\left(\frac{k^2}{4\rho_0} + \lambda\right)\right]^{\frac{1}{2}}$$

(7)

The Hamiltonian becomes

$$H = \sum_k \omega_k a^\dagger_k a_k$$

where

$$\omega_k = \frac{\sqrt{\rho_0}k}{m}\left(\frac{k^2}{4\rho_0} + \lambda\right)^{\frac{1}{2}}$$

(8)

This is nothing but the Bogoliubov spectrum. It is straightforward to show that the total

momentum operator $\vec{P}$ is $\sum_k \vec{k}a^\dagger_k a_k$. So the creation operator $a^\dagger_k$ indeed increases the total

momentum by k.

Now we include the external potential term

$$\int U(x)\rho(x)d^d x = \int U(x)\eta(x)d^d x$$

$$= \sum_k U_k(a_k + a^\dagger_{-k})\sqrt{\frac{1}{2\alpha_k}}$$

48

Call the Hamiltonian without random potential H_0, we have

$$H = H_0 + \sum_k U_k (a_k + a_{-k}^\dagger) \sqrt{\frac{1}{2\alpha_k}}$$

H can be easily diagonized by the replacements

$$b_k \equiv a_k + \xi_k \ , \ \xi_k \equiv \frac{U_k}{\omega_k \sqrt{2\alpha_k}} \tag{9}$$

and

$$H = \sum_k \omega_k b_k^\dagger b_k$$

The commutation relation between $b_k^\dagger$ and b_k is obviously the same as the one for $a_k^\dagger$ and a_k. In the following we will first calculate the superfluid density from the momentum density correlation function, then consider the phase fluctuations.

3.3 Superfluid Density and Phase Fluctuation

Let's now calculate the momentum correlation functions and the superfluid density. The momentum density operator $\vec{g}(x)$ is equal to $\frac{1}{2i}\left[\Psi^\dagger(x)\vec{\nabla}\Psi(x) - \Psi(x)\vec{\nabla}\Psi^\dagger(x)\right]$. In terms of the density and phase operators we have

$$\vec{g}(x) = \rho_0\vec{\nabla}\Phi(x) + \frac{1}{2}\left(\eta(x)\vec{\nabla}\Phi(x) + \vec{\nabla}\Phi(x)\eta(x)\right)$$

Call the first term $\vec{g}_a$ and the second term $\vec{g}_b$. The response function $R^{ij}(x,t)$ and its Fourier transform is defined by

$$R^{ij}(x,t) \equiv \; <[g^i(x,t),g^j(0,0)]> = \int \frac{d^dk\,d\omega}{(2\pi)^{d+1}} e^{i(k\cdot x - \omega\cdot t)} R^{ij}(k,\omega)$$

The susceptibility is equal to

$$\chi^{ij}(k) \equiv \int_{-\infty}^{\infty} \frac{d\omega}{2\pi}\frac{R^{ij}(k,\omega)}{\omega - i\epsilon} \equiv \frac{k^i k^j}{k^2}A(k^2) + \left[\delta_{ij} - \frac{k^i k^j}{k^2}\right]B(k^2)$$

As stated in the first chapter, $B(0)$ is the normal fluid density and the superfluid density ρ_s is the difference between the normal fluid density and the total density. As a first approximation, we consider $\vec{g}_a(x)$ only. The corresponding susceptibility is

$$\chi_a^{ij}(k) = m\rho_0\frac{k^i k^j}{k^2}$$

This clearly demonstrates the presence of superfluidity disregarding the condensate. Now we include $\vec{g}_b(x)$ and explicit calculation shows that

$$\frac{1}{m}B(0) = n_1 + n_2,$$

$$n_1 = \frac{1}{d}\int \frac{d^dp}{(2\pi)^d}p^2\frac{\partial n(\omega_p)}{\partial\omega_p}$$

$$n_2 = \frac{1}{d}\frac{1}{V}m^3\rho_0^{-1}\int \frac{<U_k^*U_k>}{\left(\frac{k^2}{4\rho_0} + \lambda\right)^2}\frac{d^dk}{(2\pi)^d}$$

(10)

50

Assuming $< U_k^* U_k >= R_0 V$, as $d = 3$ and $d = 2$ we have

$$n_2 = \frac{1}{3} \frac{1}{4\pi^{\frac{3}{2}}} m^3 R_0 \sqrt{\frac{\rho_0}{a}} \ , \ for \ d = 3 \ ; \ n_2 = \frac{1}{2} \frac{1}{4\pi^2} R_0 \frac{m^3}{a} \ , \ for \ d = 2 \qquad (11)$$

where $a = v_0 m / 4\pi$.

The 3D result is exactly the same as our previous one obtained by the Bogoliubov transformation in the second chapter. Note that at zero temperature the normal fluid density does not depend on the total particle density ρ_0 in 2D system, while it is proportional to the square root of the total density in 3D. In both cases the effect of the random potential on superfluidity becomes neglegible as the total density becomes large. At $T = 0$, the supefluid density n_s is equal to $n - n_2$, with n the total particle density. The minimal value n_c of n that gives a nonzero superfluid density is determined by the equation $n_c - n_2(n_c) = 0$. Of course our theory begins to break down before the critical value n_c is reached. However it does provide us a lower bound of n below which the disorder can not be treated as a small perturbation.

Now let us turn to the problem of condensate density and phase fluctuation. The phase fluctuation is characterized by the function

$$< [\Phi(x) - \Phi(0)]^2 > = \frac{2}{V} \sum_k [1 - \cos(kx)] \alpha_k < b_k^\dagger b_k > + \frac{1}{V} \sum_k [1 - \cos(kx)] \alpha_k \qquad (12)$$

The correlation function of the field operator can be expressed in terms of the phase fluctuation by

$$< \Psi^\dagger(x) \Psi(0) > \simeq e^{-\frac{1}{2} < [\Phi(x) - \Phi(0)]^2 >} \rho_0$$

This can be easily proved by the equivalent path integral method. In the presence of a condensate the expectation value of the field operator is finite and its autocorrelation

function above goes to some finite value as the distance $|x|$ goes to infinity. In fact $< \Psi >$ is equal to $exp(-\frac{1}{4} < [\Phi(\infty) - \Phi(0)]^2 >)$. So a finite phase difference between two remote points implies the existence of a condensate.

Note also that the random potential has no effect in the phase fluctuation to this order of approximation. This is easy to see from eq.(6) since the expression for p_k is the same in terms of a_k or b_k.

The first term in eq.(12) vanishes as the temperature goes to zero while the second term does not depend on the temperature. Unfortunately the latter suffers an ultraviolet divergence. However we believe that "zero-point" phase fluctuation should be finite in any dimension. The apparent divergence encountered here is due to the fact that our Hamiltonian is good for eigenstates with low energies only. We can not take all the k's into account unless a natural cut-off is provided, like what happened in the first term, where only low energy states contribute automatically. Since we are interested in how the fluctuation diverges when we approach a 2D system from a 3D bulk continuously, we can neglect the second term assuming it is always finite. Consider a slab and focus on the first term

$$F(L,d) \equiv \frac{2}{V} \sum_k (1 - \cos(\vec{k} \cdot \vec{L})) \alpha_k n(\omega_k) \tag{13}$$

where L is the length and width of our slab and d the thickness. The discrete momentum goes over the following values:

$$\vec{k}_{n,m,l} = \left(\frac{2\pi n}{L}, \frac{2\pi m}{L}, \frac{2\pi l}{d} \right)$$

$\vec{L}$ is an arbitrary vector of length L lying in the $x-y$ plane. $n(z)$ is equal to $1/(exp(z)-1)$. $F(L,d)$ can be separated into two terms, F_1 and F_2. F_1 is the contribution from the $l = 1$

52

modes and F_2 from the $l > 0$ modes. For given temperature T, L is assumed to be large enough such that the finite size effects in the x and y directions are neglegible. For this purpose we define a "dimensionless temperature" t to be $K_B L T / c$, where $c = \sqrt{\frac{\mu}{m}}$ is the sound velocity and $\beta = 1/K_B T$. We are interested in the region $t >> 1$. In this case the discrete sum over n and m can be replaced by a double integral. So we have

$$F_1(L,d) = 2\pi v_0 \sqrt{\frac{m}{2\mu}} \frac{1}{d} \int_0^\infty n(\beta \omega_k)(1 - J_0(kL))dk \simeq \frac{2\pi v_0}{\beta c} \sqrt{\frac{m}{2\mu}} \frac{1}{d} \ln\left(\frac{L}{2\beta c}\right) \qquad (14)$$

and

$$F_2(L,d) = \frac{2\pi}{d} \sum_{l=1}^\infty \int_0^\infty k\alpha_l(k)n_l(k)[1 - J_0(kL)]dk \qquad (15)$$

where

$$n_l(k) = n\left(\beta c (\frac{4\pi^2 l^2}{d} + k^2)^{1/2}\right) \ , \ \alpha_l(k) = \alpha\left((\frac{4\pi^2 l^2}{d} + k^2)^{1/2}\right)$$

J_0 is the bessel function. If we fix d and let L go to infinity, F_1 diverges logrithmically and F_2 stays finite. Thus the field correlation function decays by a power law, which is the characteristic feature of a 2D system. Here we take L to be large but finite and let d decrease from L. This is intended to describe the continuous transition from a bulk helium to a thin film with finite thickness. The lowest d considered here will be such that only $l = 0$ modes contribute significantly to our ensemble and all the others are not accessible by the thermal excitation. So we vary d in the interval $\frac{L}{t} < d < L$. Obviously $F_1(L,d)$ is appreciable only when d is much smaller than L, while $F_2(L,d)$ stays in some finite value when $d \sim L$ and goes to zero exponentially as $d << L$. As far as the condensate is concerned, the system is essentially three dimensional if $F_2 >> F_1$, two dimensional if $F_2 << F_1$. The square roots of F_1 , F_2 and F are depicted schematically in figure 3.1 as functions of d for fixed L.
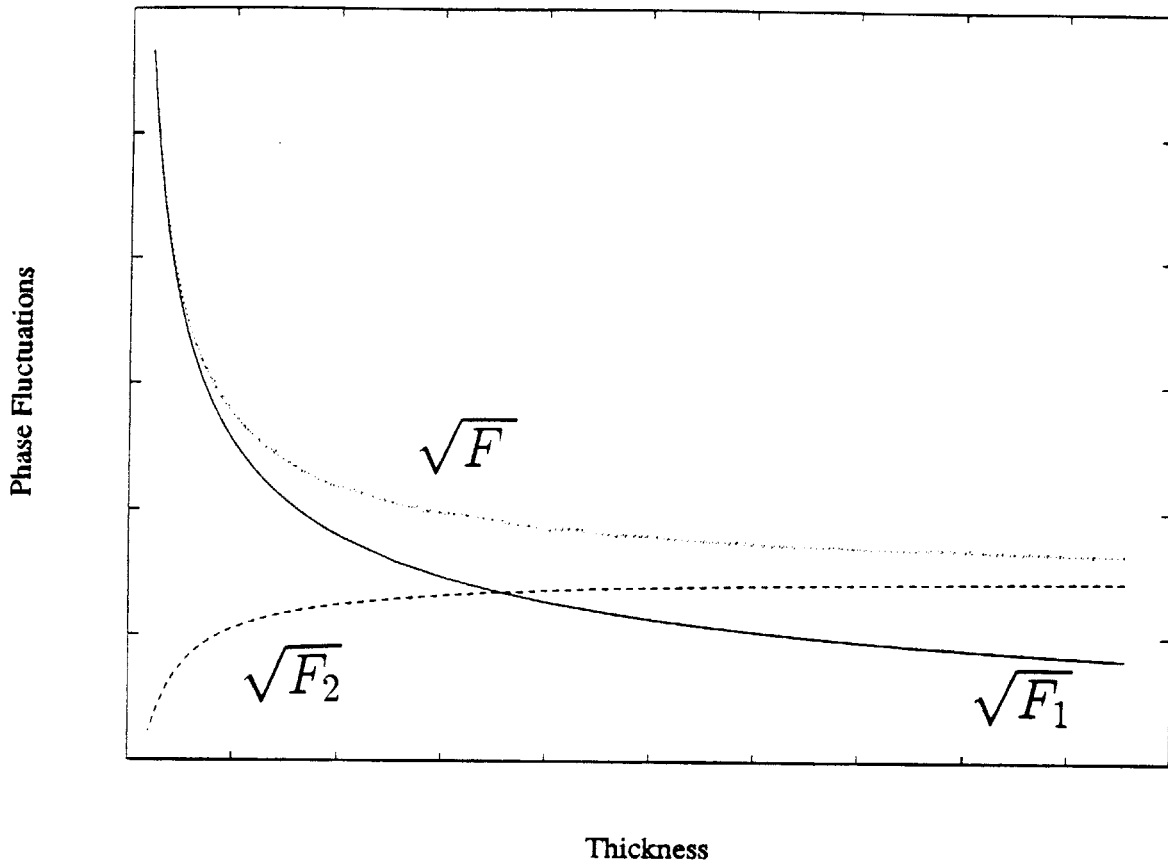
Fig. 3.1

Square roots of F, F_1 and F_2 shown as functions of the thickness d. The side length L is fixed. When d is large the system behaves like a three dimensional while it becomes more like two dimensional as d decreases. The absolute values of the axis have no particular meaning.

Let's discuss briefly how to include the vortex excitations in a 2D system. Near the superfluid transition the density fluctuation for 3D system is large due to the proliferation of large vortex rings. Therefore our method is not valid in the critical region. In 2D case we expect the theory to be valid even beyond the superfluid transition point since there are actually very few dissociated vortices at the transition temperature and the density remains essentially a constant. Path integral formalism is the natural way to include vortex excitations. The path integral equivalence to the canonical Hamiltonian is the action[5]

$$S[\Phi, \eta] = \int_0^\beta d\tau \int d^d x \left\{ \eta \left[i\frac{\partial \Phi}{\partial \tau} + U(x) \right] + \frac{1}{2m} \left[\frac{1}{4\rho_0}(\vec{\nabla}\eta)^2 + \rho_0(\vec{\nabla}\Phi)^2 \right] + \frac{v_0}{2}\eta^2 \right\} \quad (16)$$

where $\rho_0 = \frac{\mu}{v_0}$ is a constant. All the fields here are c-numbers. Define the effective action $S[\Phi]$ of Φ by

$$e^{-S[\Phi]} \equiv \int D[\eta] e^{-S[\Phi, \eta]}$$

Due to the term $(\vec{\nabla}\eta)^2$, a term proportional to $(\vec{\nabla}\frac{\partial \Phi}{\partial \tau})^2$ will be generated, which we will neglect for simplicity. This is at least valid when ρ_0 is large. After the η-integration, we have

$$S[\Phi] = \frac{\rho_0}{2m} \int_0^\beta d\tau \int d^d x \left[(\vec{\nabla}\Phi)^2 + \frac{1}{c^2}(\frac{\partial \Phi}{\partial \tau})^2 \right] \quad (17)$$

where $c = \sqrt{\frac{\mu}{m}}$ is the sound velocity. Again, all terms involving the external potential $U(x)$ drop off because the periodical boundary condition of Φ on the $\tau = 0$ and $\tau = \beta$ surfaces. This action correctly gives the linear phonon dispersion relation. Define $z \equiv c\tau$, we have in two dimension

$$S[\Phi(x, y, z)] = \frac{\rho_0}{2mc} \int_0^{c\beta} dz \int dx dy [\vec{\nabla}\Phi(x, y, z)]^2$$

55

Note that the gradient has three components. $\Phi(x, y, z)$ satifies the periodic boundary condition $\Phi(x, y, 0) = \Phi(x, y, c\beta)$. Let's decompose the 3D vector $\vec{\nabla}\Phi$ as

$$\vec{\nabla}\Phi = \vec{\nabla}\Phi_p + \vec{h}$$

The first part is the phonon part and the second the is vortex part. Φ_p is a single valued function and $\vec{h}$ is determined by the conditions : 1. $\vec{\nabla} \cdot \vec{h} = 0$. 2. The curl of $\vec{h}$ is singular at the vortex lines and zero otherwise. If the vortex lines carry d.c. electric current, $\vec{h}$ will be the magnetic field generated by them. So the action becomes

$$S[\Phi] = S[\Phi_p] + \frac{\rho_0}{2mc} \int_0^{c\beta} dz \int dx dy (\vec{h})^2 \tag{18}$$
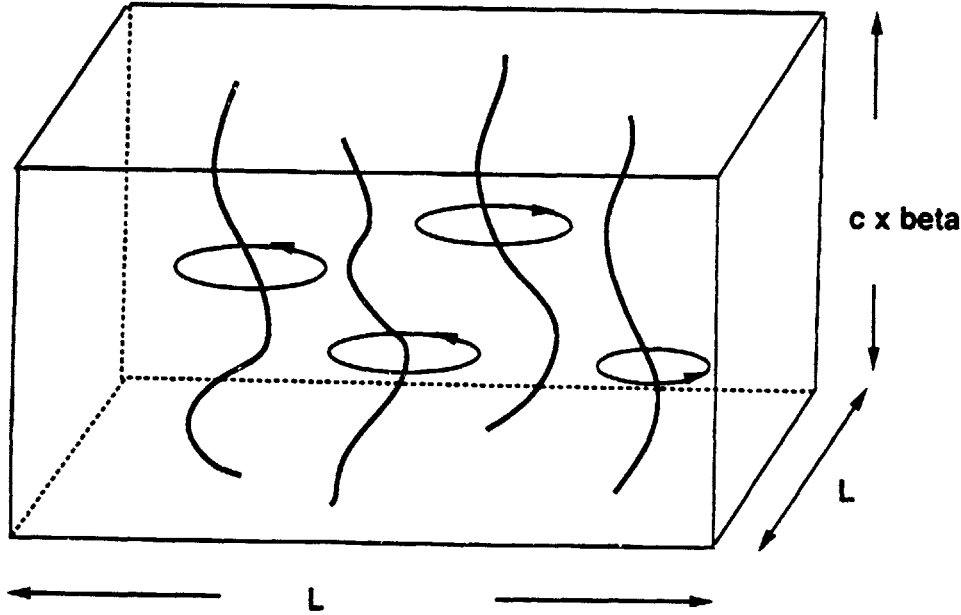
Fig. 3.2

The vortex line excitations of a two dimensional quantum system is equivelant to a classical model of three dimensional system in $L \times L \times c\beta$. The vortex rings are omited in the pictures. Note that the lines start and end up at the same point the the $L \times L$ planes.

There is no crossing term because of the condition satisfied by $\vec{h}$. $S[\Phi_p]$ can be easily diagonized in the momemtum representation. The second part is a function of the configurations of the vortex lines. The circulation of $\vec{h}$ around the lines should be a multiple of 2π since Φ is the phase. The configurations can be characterized by 1. the number of lines N, 2. the starting points ($z = 0$) of the lines $\{r_i, i = 1 \cdots N\}$, 3. the fluctuation around the straight lines $\{x_i(z), y_i(z)\}$.

This action is equivalent to a 3D classical model in a box of side length L and height $c\beta$. When β is low enough such that we can neglect the fluctuations along the z direction, we recover the KT model with r_i's the positions of the vortices (see ref. 10 of chapter one). When the temperature is low, or $c\beta$ is large, we have to consider the vortex ring excitations in addition to the lines. Also, the lines can not be taken as straight since fluctuations becomes important. However the KT theory is valid around the transition temperature as shown below.

We can decompose the fluctuations into Fourier sine series

$$x_i(z) = \sum_n A_n^i \sin(\omega_n z) \ , \ y_i(z) = \sum_n B_n^i \sin(\omega_n z)$$

where $\omega_n = \frac{\pi n}{\beta c}$. Instead of $x^i(z)$ and $y^i(z)$ we may take A_n^i and B_n^i as the degrees of freedom. Vortex rings are neglected here. When the temperature is so high such that the fluctuations around the τ-independent straight lines are small, the action separates into the vortex interaction part $S_{vi}(r_1 \cdots r_N)$ and the fluctuation part $S_f(\{A_n^i, B_n^i\})$. The core energy of the straight lines is included in S_{vi}.

The vortex interaction part is nothing but the Kosterlitz-Thouless free energy. As long as the condition for this decomposition is valid, the second part only give a temperature

dependent core size for the KT model which is known to be unimportant. In that case the KT theory is correct as a microscopic theory. Our aim here is to exam when this decomposition begins to break down. An obvious criterion is whether the size of the fluctuation is larger than the height of the vortex lines. If it is true then there is no reason that we can neglect the vortex rings since they can easily grow out of a strongly distorted line and the positions r_i's of the vortices are not enough to describe the system. The size of the fluctuation is equal to $\Delta \equiv \sqrt{< x^2 + y^2 >}$. The index i is omitted here, assuming the vortex lines are roughly independent. The fluctuation action $S_f(A_n, B_n)$ for some particular line is the increase of the energy due to the change of the total length of it and equals

$$S_f = \frac{\beta c E_c}{4} \sum_{n=1}^{\infty} \omega_n^2 (A_n^2 + B_n^2)$$

,where E_c is the core energy per unit length. The dimensionless chemical potential of the vortices in the KT theory $\ln(y)$ is equal to $-\beta c E_c$. It is related to the dimensionless temperature $K \equiv \rho_o \beta / m^2$ by $\ln(y) = -\frac{1}{2}\pi^2 K$ [6]. After straightforward calculation we find

$$\Delta = \frac{2}{\pi^2} \sqrt{\zeta(2)} \frac{\beta c}{K^{1/2}} \simeq 0.37 \frac{\beta c}{K^{1/2}}$$

The condition for the KT theory to be valid is $\Delta \leq \beta c$. In other words

$$\frac{1}{K} \leq 7.3$$

Near the transition point K is roughly one [6], so the KT theory is correct to describe the helium film phase transition for all the surface densities.

58

3.4 Application to Fractional Quantum Hall Effect

Fractional quantum Hall effect is probably the most interesting property of two dimensional electron gas in a strong perpendicular external magnetic field. The most important physical quantity is the off-diagonal d.c. conductivity σ_H. σ_H is equal to $\nu\frac{e^2}{2\pi}$ when the filling number ν is equal to $\frac{1}{2k+1}$, with k a positive integer. Here we set the units such that $c = 1$, $h = 2\pi$.

One of the most successful microscopic theories is the so-called Chern-Simons-Laudau-Ginzburg theory [3]. In this theory the original 2D fermion problem is mapped by the anyon method [7] into a boson problem coupled to a Chern-Simons gauge field. In the following we will show that the boson Hamiltonian for FQHE can be diagonized without the introduction of the auxilary Chern-Simons term. The off-diagonal conductivity will be calculated and is reduced to the well-known value $\nu\frac{e^2}{2\pi}$ at the static limit. The effect of finite temperature and random external potential will also be discussed.

Let's start with the boson second quantized Hamiltonian of FQHE [1].

$$
\begin{aligned}
H =& \frac{1}{2m} \int d^2 r \Psi^\dagger (-i\vec{\nabla} - e\vec{A} - e\vec{a})^2 \Psi - \mu \int d^2 r \Psi^\dagger \Psi \\
&+ \frac{1}{2} \int d^2 r d^2 r' \Psi^\dagger(r)\Psi^\dagger(r')V(r - r')\Psi(r)\Psi(r') \\
=& H_0 + H_1
\end{aligned}
\tag{19}
$$

As before, we can expand the density operator ρ around its mean value $\bar{\rho}$. Keep up to the quadratic terms we have

$$
H_0 = \frac{1}{2m} \int d^2 r \left[\frac{1}{4\bar{\rho}}(\nabla\eta)^2 + \bar{\rho}(\nabla\Phi)^2 \right] + \frac{1}{2} \int d^2 r d^2 r' \eta^\dagger(r)V(r - r')\eta(r')
$$

$$H_1 = -\frac{e}{m} \int d^2r(\vec{A} + \vec{a}) \cdot \vec{J} + \frac{e^2}{2m} \int d^2r(\vec{A} + \vec{a})^2\rho$$

$\vec{A}$ generates the static perpendicular magnetic field. $\vec{J}$ is equal to $\rho\vec{\nabla}\theta$. $\vec{a}$ is determined by ρ through [8]

$$\epsilon^{\alpha\beta}\partial_\alpha a_\beta(x) = \phi_0 \frac{\theta}{\pi}\rho(x)$$

$$\partial^\alpha a_\alpha(x) = 0$$

(20)

θ should be π times some odd integer. ϕ_0 is the unit flux hc/e. The left hand side of the first equation is actually the z component of the curl of $\vec{a}$. We can image that $\vec{a}$ is obtained by associating a unit flux tube to each boson. When the filling number ν is equal to $1/(2k+1)$, we can chose θ to be π/ν. In this case $\vec{A}$ and the part of $\vec{a}$ generated by the constant mean value $\bar{\rho}$ have equal magnitudes and opposite signs. So $\vec{A} + \vec{a}$ is of the order of η, the density fluctuation. In fact, in terms of the Fourier components we have

$$A_\alpha(k) + a_\alpha(k) = \frac{2\theta}{e}\epsilon^{\alpha\beta}\frac{ik_\beta}{k^2}q_k$$

(21)

and

$$H_0 = \frac{1}{2m}\sum_k \left(\frac{k^2}{4\bar{\rho}} + mV(k)\right)q_k q_{-k} + \bar{\rho}k^2 p_k p_{-k}$$

Again, up to the quadratic terms

$$H_1 = \frac{2\bar{\rho}\theta^2}{m}\sum_k \frac{1}{k^2}q_k q_{-k}$$

Combine H_0 and H_1, we get

$$H = \frac{1}{2m}\sum_k \left(\frac{k^2}{4\bar{\rho}} + \lambda_k\right)q_k q_{-k} + \bar{\rho}k^2 p_k p_{-k}$$

with

$$\lambda_k = mV(k) + \frac{4\pi^2\bar{\rho}}{\nu^2 k^2}$$

60

This Hamiltonian can be diagonized in almost the same way as the superfluid. The only difference is that now λ_k is not a constant. The new expressions for α_k, ω_k and ξ_k can be obtained by replacing the λ's in the old expressions by the λ_k given above. In particular, the square of the new spectrum is found to be

$$
\begin{aligned}
\omega_k^2 &= \frac{\bar{\rho}k^2}{m^2}\left(\frac{k^2}{4\bar{\rho}} + \lambda_k\right) \\
&= \omega_c^2 + \frac{1}{m}\bar{\rho}k^2 V(k) + \frac{1}{4m^2}k^4
\end{aligned}
\tag{22}
$$

with

$$
\omega_c = \frac{2\pi\bar{\rho}}{m\nu}
$$

This shows that the spectrum has an energy gap, typical for an imcompressible liquid.

In order to study the linear response of this system to an external perturbation, we turn on a small extra vector potential $\vec{A}_1(r,t)$. The gauge invariant physical electric current density $\vec{J}$ is equal to $\vec{J}_1 + \vec{J}_2 + \vec{J}_3$ where

$$
\vec{J}_1 = \frac{e}{m}\rho\vec{\nabla}\theta
$$

$$
\vec{J}_2 = -\frac{e^2}{m}[\vec{A} + \vec{a}]\rho
$$

$$
\vec{J}_3 = -\frac{e^2}{m}\vec{A}_1\rho
$$

The interaction Hamiltonian H_I due to $\vec{A}_1$ is

$$
H_I = -\int d^2r\left(\vec{J}_1 + \vec{J}_2\right)\cdot\vec{A}_1
$$

We can use the Kubo formula to evaluate the linear response function. Since there are three terms in the electric current and two terms in the interaction Hamiltinian, we get totally six commutators. However only the following two contribute to the off-diagonal conductivity :

$$
\sigma_1^{\alpha\beta}(r,t) \equiv i\theta(t) < [J_2^\alpha(r,t), J_1^\beta(0,0)] >
$$

61

$$\sigma_2^{\alpha\beta}(r,t) \equiv i\theta(t) < [J_1^\alpha(r,t),\, J_2^\beta(0,0)] >$$

The Fourier transforms of them give the linear response functions. Let's calculate $\sigma_1^{\alpha\beta}(k,\omega)$ first.

$$
\begin{aligned}
J_2^\alpha(k,t) =& \frac{e^2}{m}\frac{2\theta}{e}\bar{\rho}\epsilon^{\alpha\beta}\frac{ik_\beta}{k^2}q_k(t) \\
&+ \frac{e^2}{m}\frac{1}{V}\frac{2\theta}{e}\epsilon^{\alpha\beta}\sum_{k'}\frac{ik'_\beta}{k'^2}q_(k',t)q_(k'+k,t)
\end{aligned}
$$

Similarly,

$$
\begin{aligned}
J_1^\alpha(k,t) =& \frac{e}{m}\bar{\rho}ik^\alpha p_{-k}(t) \\
&+ \frac{e}{m}\frac{1}{V}\sum_{k'}i(k'+k)^\alpha q_{k'}(t)p_{-k'-k}(t)
\end{aligned}
$$

From the above expressions we have

$$
\begin{aligned}
\sigma_1^{\alpha\beta}(k,t) =& i\theta(t) < [J_2^\alpha(k,t),\, J_1^\beta(-k,0)] > \\
=& \frac{e^2}{m}\frac{2\theta}{e}\bar{\rho}\epsilon^{\alpha\gamma}\frac{ik_\gamma}{k^2}\frac{e}{m}\bar{\rho}(-i)k_\beta < [q_k(t),\, p_k(0)] > \\
&+ \frac{2e^2\theta}{m^2 V}\epsilon^{\alpha\beta}\sum_{k',k''}\frac{ik'_\gamma}{k'^2}i(k''-k)_\beta < [q_{k'}(t)q_{k'+k}(t),\, q_{k''}(0)p_{k-k''}(0)] >
\end{aligned}
$$

The first term is easy to calculate using

$$< [q_k(t),\, p_k(0)] > = \frac{i}{2}(e^{i\omega_k t} + e^{-i\omega_k t}).$$

In order to get the electric conductivity we have to make the temporal Fourier transform then divide it by $i\omega$ remembering that $\vec{E}(k,\omega) = i\omega\vec{A}(k,\omega)$. Similarly we can calculate $\sigma_2^{\alpha\beta}(k,\omega)$. It also separates into two parts, one involving only two operators and another involving four. Combine $\sigma_1^{\alpha\beta}(k,\omega)$ and $\sigma_2^{\alpha\beta}(k,\omega)$ and neglect terms involving four opera-

tors we get the final result

$$\sigma^{\alpha\beta}(k,\omega) \equiv \frac{1}{i\omega}(\sigma_1^{\alpha\beta}(k,\omega) + \sigma_2^{\alpha\beta}(k,\omega))$$
$$= \frac{e^3}{m^2}\bar{\rho}^2\frac{2\theta}{e}\frac{1}{\omega_k^2 - \omega^2}\left(\epsilon^{\alpha\gamma}\frac{k_\gamma k_\beta}{k^2} - \epsilon^{\beta\gamma}\frac{k_\gamma k_\alpha}{k^2}\right) \qquad (23)$$
$$= \frac{2e^2\theta}{m^2}\bar{\rho}^2\frac{1}{\omega_k^2 - \omega^2}\epsilon^{\alpha\beta}$$

As $\omega \to 0$, we have

$$\sigma^{\alpha\beta}(k,0) = \frac{e^2}{2\pi}\nu\epsilon^{\alpha\beta} \qquad (24)$$

Thus we derived the Hall conductivity from the first principle. Clearly to this order there is no effect coming from the finite temperature and the random potentials. Explicit evaluation of the terms involving the porduct of four operators shows that the lowest order correction from those effects is of the order of k^2. It means they have no effect at $k \to 0$ limit as it should be. This is consistent with the observation that the expression above for the Hall conductivity is exact. In other words, it is insensitive against small temperature variations and small amount of impurities.

This derivation of the Hall conductivity and the excitation spectrum of FQHE is conceptually simpler than the Chern-Simons-Laudau-Ginzburg theory. In addition, we are able to cover with ease the case of finite temperaure, while the original Chern-Simons-Laudau-Ginzburg theory is restricted to zero temperature. The prelimary test of our method indeed shows that it agrees with the well-known results. One should not be surprised since these two theories are in fact different ways to approximate the same Hamiltonian. However the regions of validity could be different. In particular, the role of vortex excitations and the ability to construct the hierarchical wave functions have not been clear and demand further study.

3.5 Strongly Disordered Superfluid

The previous results are valid only when the density $< \rho(x) >$ is approximately a constant, which is true when the energy scale of the external potential is small compared with the self-interactions. As we have seen, a system under such a condition is always a superfluid at zero temperature, even though the superfluid density is in general smaller than the total density. In order to study the strongly disordered system we need a different approach to the problem. It turns out that the path integral method is the most convenient way to formulate our theory.

For a given external potential $U(x)$ we can use the saddle point approximation to evaluate the density distribution $\rho_0(x) \equiv< \rho(x) >$ which has strong spatial dependence when the total particle density is low. Given $\rho_0(x)$, we can again expand the density up to the second order around it and evaluate the Green's functions.

The partition function Z is

$$Z = \int D[\Psi] e^{-S[\Psi, \Psi^*]}$$

where the action S is

$$S = \int_0^\beta d\tau \int d^d x \Psi^* \left(\frac{\partial}{\partial \tau} - \frac{\nabla^2}{2m} - \mu + U(x) \right) \Psi + \frac{v_0}{2} \int_0^\beta d\tau \int d^d x (\Psi^* \Psi)^2$$

Let $\Psi(x) = \sqrt{\rho(x)} e^{i\Phi(x)}$, the action becomes

$$S[\rho, \Psi] = \int_0^\beta d\tau \int d^d x \left\{ i\rho \frac{\partial \Phi}{\partial \tau} + \frac{1}{2m} \left[\frac{1}{4\rho} (\vec{\nabla} \rho)^2 + \rho(\vec{\nabla} \Phi)^2 \right] + (-\mu + U(x))\rho + \frac{v_0}{2} \rho^2 \right\}$$

$$(25)$$

The saddle point solution is determined by

$$\frac{\delta S}{\delta \rho} = 0 \ , \ \frac{\delta S}{\delta \Phi} = 0$$

From the expression for S, we have

$$i\frac{\partial \Phi}{\partial \tau} - \frac{1}{2m}\left[\frac{1}{2}\vec{\nabla}\left(\frac{1}{\rho}\vec{\nabla}\rho\right) + (\vec{\nabla}\Phi)^2\right] + (U(x) - \mu) + v_0\rho = 0$$

$$-i\frac{\partial \rho}{\partial \tau} - \frac{1}{m}\vec{\nabla}(\rho\vec{\nabla}\Phi) = 0$$

It is clear that the solution $\{\rho(x), \Phi(x)\}$ that minimizes the action satisfies the conditions
: 1. They have no τ dependence. 2. $\vec{\nabla}\Phi = 0$. So the above equations are reduced to

$$-\frac{1}{2}\frac{1}{2m}\vec{\nabla}\left(\frac{1}{\rho}\vec{\nabla}\rho\right) + (U(x) - \mu) + v_0\rho = 0 \tag{26}$$

Obviously the solution of this equation can not change sign due to the $1/\rho$ term. This guarantees the positivity of ρ. We can write $\rho(x) = \rho_0(x) + \eta(x)$ where $\rho_0(x)$ is the saddle point solution. Substitute it into the action and keep η up to the second order we have

$$S = S[\rho = \rho_0, \Phi = 0] + S_1[\eta, \Phi] + higher \ order \ terms$$

The quadratic term S_1 is equal to

$$S_1 = \int_0^\beta d\tau \int d^d x \left\{ i\eta\frac{\partial \Phi}{\partial \tau} + \frac{1}{2m}\left[\frac{1}{4\rho_0}(\vec{\nabla}\eta)^2 + \rho_0(\vec{\nabla}\Phi)^2\right] + \frac{v_0}{2}\eta^2\right\}$$

Remember that ρ_0 is a function of x. Here we assumed $\rho_0(x)$ varies slowly in space and throw away terms involving $\vec{\nabla}\rho_0(x)$. In the following we consider a simple 2D case only. Assume that $U(x)$ is composed of a set of potential wells located at the lattice sites of a square lattice with lattice spacing b. The solution $\rho_0(x)$ is of course also a periodic function with the same discrete translational symmetry as $U(x)$. Let's imagine

65

a real space renormalization up to length scale b. In other words, for the configurations $\{\Phi_i(\tau), \eta_i(\tau)\}$ on the lattice, with i the site index, we have an effective action which recovers a homogeneous continuum limit for length scales much larger than b

$$\bar{S}_1[\Phi, \eta] = \int_0^\beta d\tau \int d^d x \left\{ i\eta \frac{\partial \Phi}{\partial \tau} + \frac{1}{2m} \left[\frac{1}{4\rho_1} (\vec{\nabla}\eta)^2 + \rho_2 (\vec{\nabla}\Phi)^2 \right] + \frac{v_1}{2}\eta^2 \right\}$$

Here ρ_1, ρ_2 and v_1 are the renormalized coupling constants. They should not depend on the position because all the lattice sites are completely equivalent. Higher order terms generated by course graining are neglected. The explicit calculation of ρ_1, ρ_2 and v_1 is obviously extremely difficult, if possible. However the interesting thing is that in the the strongly disordered case where the particles are strongly localized, we can approximate ρ_2 by the value of $\rho_0(x)$ half-way between the neighboring lattice sites. Furthermore, ρ_1 does not enter the final expression of the superfluid density at zero temperature, which is in fact simply ρ_2 as we have seen in Section 3.3 . When the total particle density is small, $\rho_0(x)$ inside the potential well is much larger than it outside. Because of the $\rho_0(x)[\vec{\nabla}\Phi(x)]^2$ term in the original action, for given choice of the lattice site phase values $\{\Phi_i\}$, the only configuration that has a siginificant contribution in the renormalization is the one that is essentially constant inside the potential well and changes uniformly between the neighboring sites. So $\int \rho_0(x)[\vec{\nabla}\Phi(x)]^2 d^2 x$ can be replaced by $\sum_{n.n.} \bar{\rho}(\frac{\Phi_i - \Phi_j}{b})^2 b^2$. $n.n.$ means the nearest neighbors. $\bar{\rho}$ is the average value of $\rho_0(x)$ outside the potential well. For length scales much larger than b, we have

$$\bar{\rho} \sum_{n.n.} (\Phi_i - \Phi_j)^2 \simeq \bar{\rho} \int (\vec{\nabla}\Phi)^2 d^2 x$$

So we find the superfluid density $\rho_s = \rho_2 \simeq \bar{\rho}$. For given μ in priciple we can solve eq.(26) and obtain both the total density and the superfluid density.
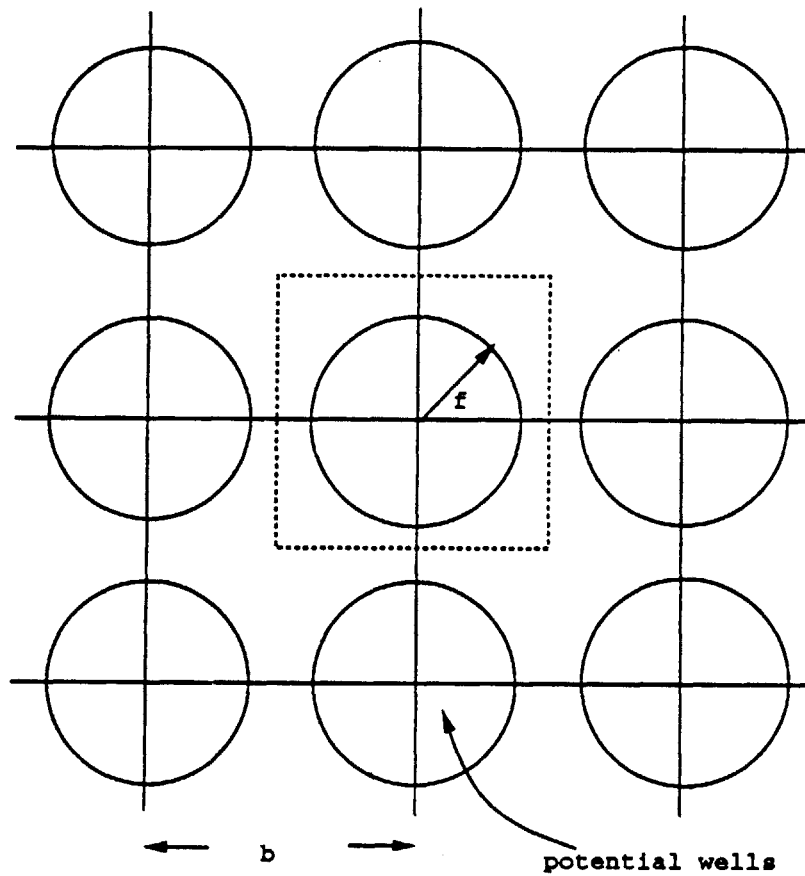
66

Fig. 3.3

This is a simple chioce of $U(x)$. Inside the circles are potetial wells of depth c. Due to symmetry

requirement we only need to know the value of ρ inside the dashed rectangle. b is the lattice spacing.

For an irregular $U(x)$, the numerical computation of the solution of eq.(26) could be very difficult since it is nonlinear. Instead of considering an irregular potential, we choose $U(x)$ to be as simple as possible. We believe that the natural of the localization does not depend on the detailed structure of $U(x)$. Our choice of $U(x)$ is a set of circular potential well of depth c and radius f, located at the sites of a square lattice with lattice spacing b (figure 3.3).

We only need to solve $\rho(x)$ in the dashed region and impose the periodic boundary condition that $\rho(x)$ has to be the same in the opposite sides. $\rho(x)$ should be maximal at the site centers and forms a valley along the sides due to the reflection symmetry. We make a further approximation to replace the b.c. on the square sides to be a b.c. on a circle of similar size. After this replacement the approximate solution becomes circular symmetrical and the differential equation of eq.(26) is transformed into an one dimensional one. The circle of the boundary condition is shown in figure 3.4.

This replacement is valid only when the solution is essentially a constant in an annal covering the square sides. Our numerical calculation shows that it is indeed the case.

Let r be the distance from the site to a point. ρ is now a function of r only. Define $u \equiv \ln(\rho)$, the equation for $u(r)$ becomes

$$-\frac{1}{2}\left(\frac{du^2}{dr^2} + \frac{1}{r}\frac{du}{dr}\right) + U(r)c + v_0 e^u = 0 \qquad (27)$$

where $\theta(t) = \theta(r - f) - 1$ is the step function. The potential $U(r)$ is shown in figure 3.5.

μ is used to control the total particle density n. It turns out that $n \rightarrow 0$ as μ approaches some finite negative value.

Circle A of boundary
conditions
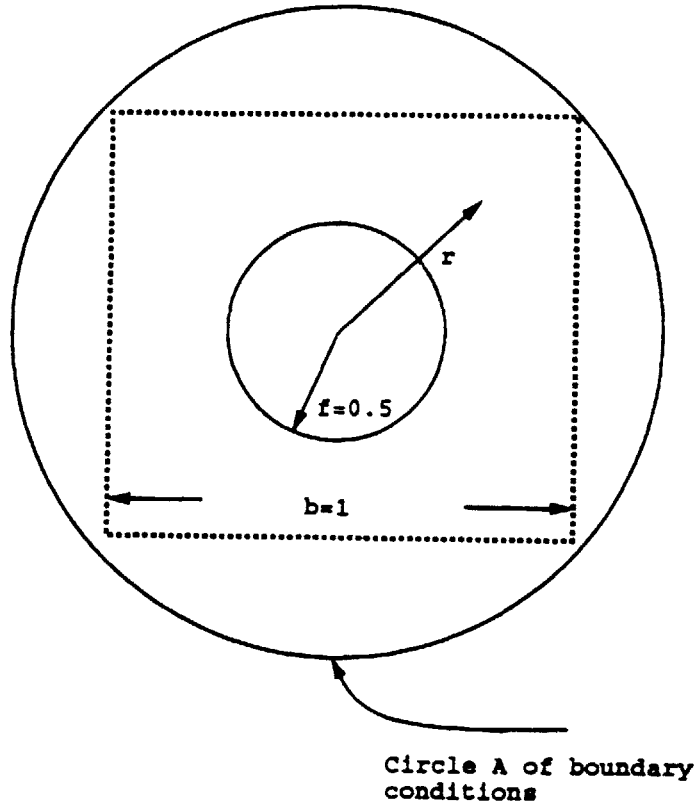
Fig. 3.4

Boundary condition is imposed on the outside circle instead on the dashed rectangle.

Figure 3.6 shows the r-dependence of the solution $\rho(r)$ for various μ's. The total

particle density ρ_t is the average of $\rho(r)$ inside the dashed line in fig. 3.3. We see that ρ

varies slowly near the boundary. This justifies our assumption that the boundary condition

can be replaced to be on the circle. Figure 3.7 is a local maginification of fig. 3.6. We find

that for large μ, ρ remains a finite value outside the well. In fact, the difference between

the density inside and outside becomes less and less obvious as the total particle density gets larger and larger. On the contrary, for small μ, or small total particle density, the density outside the well becomes strongly depressed.
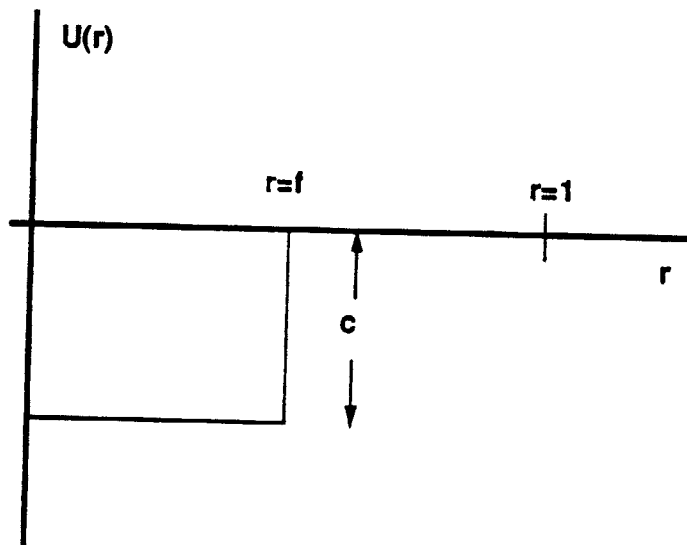
Fig. 3.5

The external potential U in the circular approximation. r is the distance to the lattice site.

Figure 3.8 is the plots of the total particle density ρ_t and the superfluid density $\rho_s = \bar{\rho}$ as functions of μ. Note that ρ_s approaches zero much faster than ρ_t. Figure 3.9 is a plot ρ_s as a function of ρ_t. The plot in figure 3.10 is superfluid *fraction* against the total fluid density. The interesting thing is that the fraction goes to zero instead of a finite number. This can be viewed as some kind of localization which gets stronger and stronger as we

70

reduce the total density. In the limit $\rho_t \to 0$, the fluid becomes completely localized and the superfluid nature is totally destroyed by the external potential.
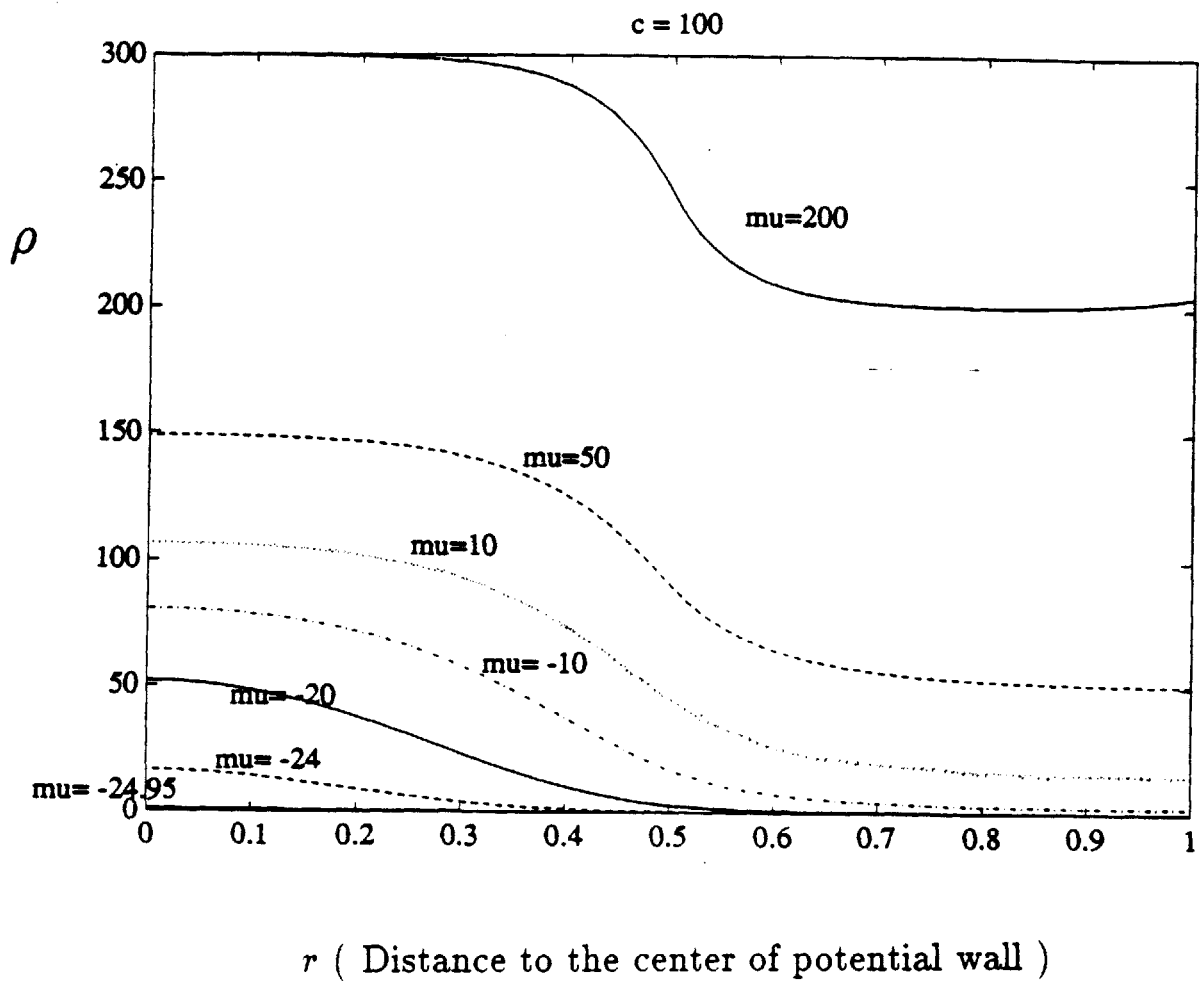
Fig. 3.6

Plots of particle density distribution $\rho(r)$ for various μ's
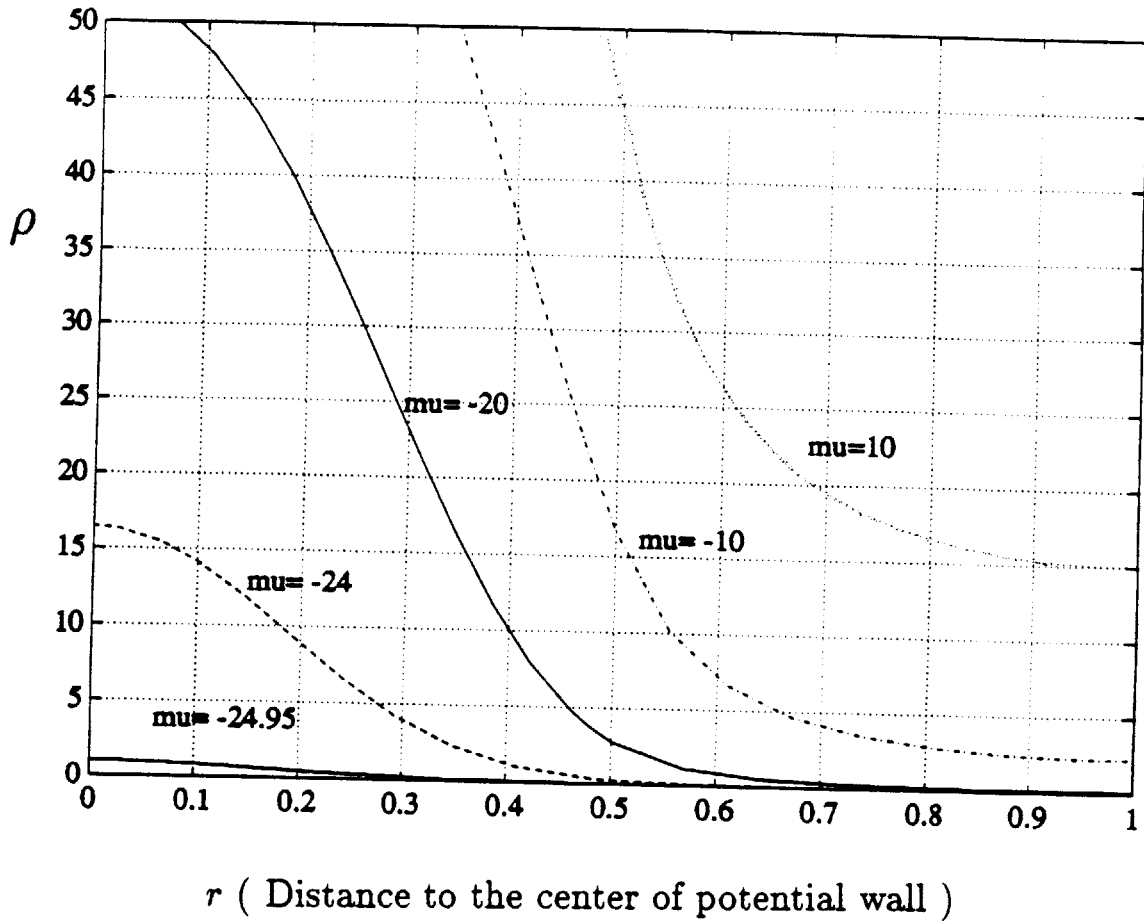
Fig. 3.7

Local maginification of fig. 3.6. We find that for large μ, $\rho(r)$ remains finite values outside the well. On the contrary, for small μ, or small total particle density, the density outside the well becomes strongly depressed.

In the present model, even though we do see a sign of boson localization, there is no abrupt phase transition observed. It is also not likely that the next order approximation will make a qualitative difference and exhibit a transition. We believe that the experimental

fact that helium thin film has no superfluidity when the total density is below some critical value dose not necessarily mean that the 2D interacting boson model contains a phase transition. As stated in the introduction chapter, the liquid helium film is actually neither purely 2D nor purely 3D. In order to understand its properties, especially the transition, we should take into acount the different roles of the successive layers in the film. A full theoretical study of this is out of the scope of this thesis.
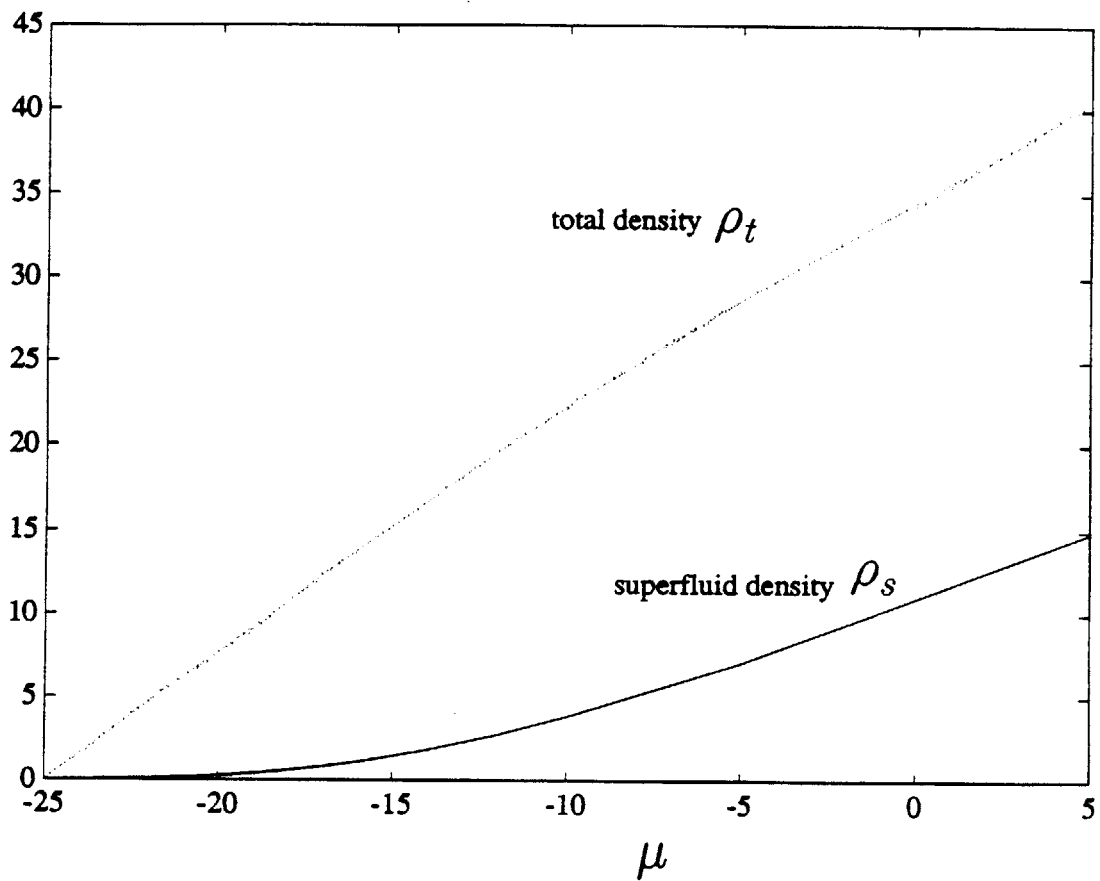
Fig. 3.8

The plots of total particle density ρ_t and the superfluid density $\rho_s = \bar{\rho}$ as functions of μ. Note that ρ_s approaches zero much faster than ρ_t.

74
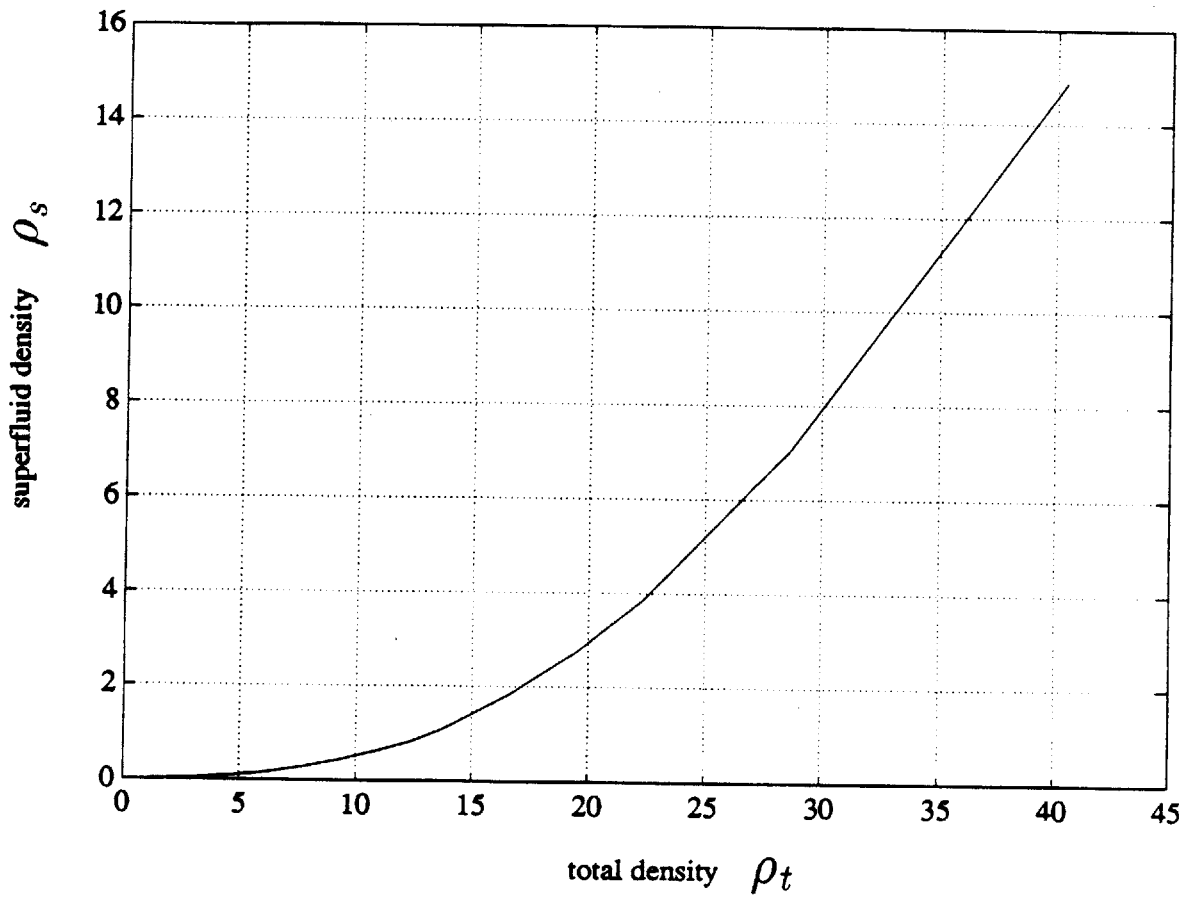
Fig. 3.9

Plots ρ_s as a function of ρ_t.
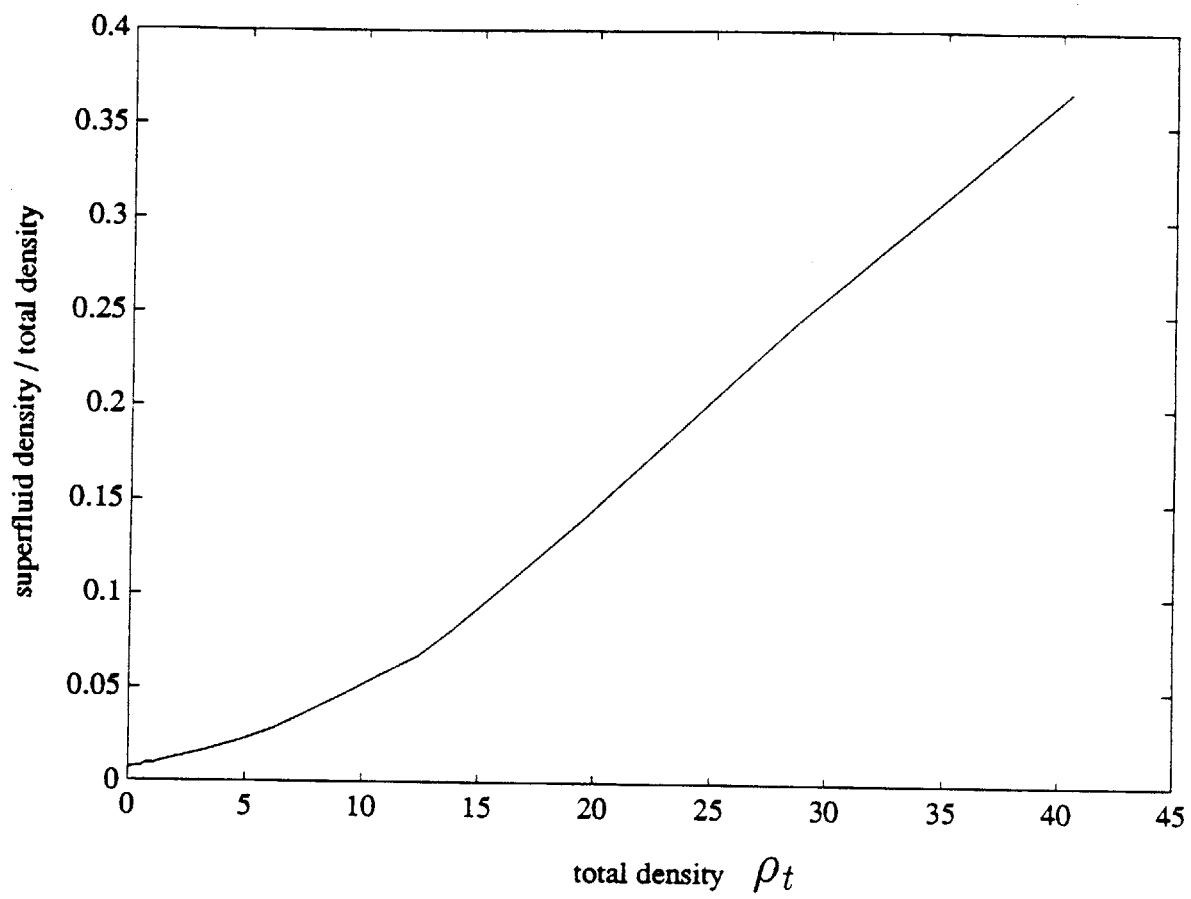
Fig. 3.10

The superfluid *fraction* against the total fluid density. The interesting is that the fraction goes to

zero instead of some constant.

76

References

[1] S.C. Zhang, T.H. Hansson and S. Kivelson, Phys. Rev. Lett., **62**, 82 (1988).

[2] K. Huang and C.N. Yang, Phys. Rev. **105**, 767 (1957)

[3] *The Quantum Hall Effect*, edited by R.E. Prange and S.M. Girvin (Springer-Verlag, 1988)

[4] K. Huang and H. Meng, Phys. Rev. Lett., **69**, 644 (1992).

[5] V.N. Popov, *Functional Integrals in Quantum Field Theory and Statistical Mechanics*, (D. Reidel Pub. 1983)

[6] S. Solla and E. Riedel, Phys. Rev. B **23**, 6008 (1981).

[7] D.P. Arovas, J.R. Scrieffer, F. Wilczek and A. Zee, Nucl. Phys. **B251**, 117 (1985).

[8] S.C. Zhang, International Journal of Modern Physics B, **6**, 25, (1992)

Chapter Four

Superfluid Helium in Disordered Media at Full Pore

The flow of superfluid ^{4}He through sponge-like media at full pore is modeled by the flow of current through an ohmic network with random resistors. Computer simulations show that the superfluid critical point is a percolation threshold, with critical exponent 1.7. The fractal dimension of the percolating cluster is 2.6, which, by Josephson's hyperscaling relation, implies a specific heat exponent $\alpha = -5.4$. Existing experiments apparently do not cover the critical region. Instead, they measure "mean-field" exponents, whose values for Vycor, aerogel, and xerogel can all be reproduced by choosing appropriate distribution functions for the resistors.

4.1 Model of Simulation

There have been many experimental studies of superfluid ^{4}He adsorbed in the sponge-like media Vycor, aerogel, and xerogel, with porosities ranging from 30% to 96% [1]-[4]. The superfluid density and specific heat have been measured, for wide ranges of coverage, from a few atomic layers to full pore, and for wide ranges of temperature below the lambda point of bulk liquid helium. The superfluid transition temperature is found to decrease with decreasing coverage, extrapolating to zero at a nonzero critical coverage. Thus, superfluidity disappears below a critical coverage, even at absolute zero. Near the critical coverage, the superfluid exponent has the ideal-gas value $\zeta = 1$. When the coverage is increased from the critical value, however, different physics takes over at some point, for

ζ is observed to cross over to a different value. At full pore, the ζ for Vycor, and xerogel are respectively 0.67 and 0.89 [2]. For aerogel, the values are 0.80 according to [2], and 0.75 according to [4]. For comparison, $\zeta = 0.672$ for the bulk liquid. In an earlier work [5], we demonstrated the disappearance of superfluidity at absolute zero in a dilute hard-sphere Bose gas in random potentials, due to boson localization, i.e., pinning of the Bose condensate by the random potentials. In this paper, we consider the full-pore case, and propose a model that can explain some of the observations in that regime.

We model the flow channels in the sponge-like medium as bonds in a cubic lattice, with channel radii chosen at random from a given distribution. We have considered two types of distributions: a Gaussian distribution with adjustable center and width, and a uniform distribution with adjustable lower and upper cutoffs. In either case, the medium is characterized by two parameters.

In a long channel of radius r at full pore, the superfluid transition temperature $T_c(r)$ decreases with r, for large r, according to a power law [6]:

$$1 - T_c(r)/T_\infty \approx (r/r_0)^{-q}, \tag{1}$$

where $q \approx 2$, $r_0 \approx 5nm$, and $T_\infty = 2.172\ K$ is the bulk transition temperature. We use a simply interpolation formula for all r: $T_c(r)/T_\infty = 1 - [1 + (r/r_0)^q]^{-1}$. The superfluid density in a channel of radius r at temperature T, denoted by $\rho_s(r, T)$, is of course zero for temperatures $T > T_c(r)$. For $0.9 < [T/T_c(r)] < 1$, we take

$$\rho_s(r, T) = K_1[1 - T/T_c(r)]^\xi, \tag{2}$$

where $\xi = 0.67$ is the bulk critical exponent, and K_1 a constant. Outside of the indicated interval we use a polynomial form that reduces to $1 - K_2 T^2$ near $T = 0$, and joins smoothly

on to the formula above. Our results are not sensitive to how we interpolate. The channel lengths are effectively infinite. How realistic this assumption is will be discussed later.

The momentum density for superfluid flow is given by $\mathbf{j} = \rho_s \mathbf{v}_s + \rho_n \mathbf{v}_n$, where the two terms refer to the superfluid and normal fluid, respectively. Assuming that all channels are so small that the normal fluid is pinned, we put $\mathbf{v}_n = 0$. Thus, writing $\mathbf{v}_s = \nabla \phi$, where ϕ is proportional to the superfluid phase, we have

$$\mathbf{j} = \rho_s \nabla \phi. \tag{3}$$

This looks like Ohm's law with current density $\mathbf{j}$, electrostatic potential ϕ, and electrical conductivity ρ_s. Thus, each bond can be replaced by a resistor, and the superfluid density of the medium corresponds to the conductivity of the network. Because of the close analogy, we shall freely use the language of the electrical analog when convenient.

After assigning the bond radii, and with that the electrical resistances, we calculate the conductivity of the network by solving Kirchoff's equations on a computer, using Gauss-Seidel iteration with SOR (Simultaneous Over-Relaxation) [7]. We use lattice sizes 10^3 and 20^3, with some calculations done on 30^3 and 50^3 lattices. In the following, we summarize the insight gained from the computer simulations, illustrated with plots of quantitative results, and conclude with some critical remarks.

4.2 Results

Imagine that a voltage (superfluid phase) difference is established between the top and bottom plates of the lattice, taken to be equipotentials. At high temperature all channels are closed, and the network is non-conducting (no superfluid flow.) As the temperature is lowered, some channels become conducting, but the whole network remain non-conducting until a percolating cluster of open bonds connects the top to the bottom plate. The percolation threshold T_0 (which is not the T_c of the experiments,) is the true critical point for the onset of superfluidity. The behavior near this threshold, in a finite lattice, has a complicated structure. When the temperature is increased, opening up a single bond can appreciably enlarge the percolating cluster. As a result, the superfluid density exhibits a series of bumps with discontinuous derivatives. The slope at the beginning of each bump corresponds approximately to the bulk critical exponent ζ, which is an input to the calculation. This behavior is illustrated in Fig.4.1a, where the cluster size, as well as the fraction of open channels, are also shown. When we go to a larger lattice, the bumps in the superfluid density tend to be smoothed out. The critical exponent ζ_0 for an infinite lattice can be approximately calculated by averaging over these bumps. We obtain in this fashion $\zeta_0 \approx 1.7$, which agrees with numerical results on percolation in 3D [8].

The specific heat at percolation threshold behaves like

$$C = (A/\alpha)|T_0 - T|^{-\alpha} + B, \tag{4}$$

where A and B are constants. Josephson hyperscaling [9] predicts $\zeta_0 d = (2-\alpha)(d-2)$. Using $\zeta_0 = 1.7$ and $d = d_f = 2.6$, we obtain for the specific heat exponent $\alpha = -5.4$, which makes it difficult to detect the singularity experimentally. Specific heat peaks were observed in aerogel at full pore in Ref.[3], which also reports slight shifts of T_0 in different samples of aerogel cut from the same block. The latter can be explained by the dependence of the percolation threshold on pore distribution. The peaks observed in [3] are probably due to crossover to a "mean-field" region discussed below, the true critical region being buried in the sharp rise of the specific heat.

When the temperature is decreased from the percolation region, the system crosses over to a "mean-field" regime, in which the superfluid density has a different power-law behavior, with exponent ζ. This is shown in Fig.4.1b, in a zoom-out from the previous picture, and the process is continued in Fig.4.2. The mean-field region corresponds to that studied extensively in experiments, while the crossover region corresponds to the "tails" in the data that have always been ignored.

The difference between the mean-field and the critical region is revealed by measuring the fractal dimension d_f of the percolating cluster in the computer. As shown in Fig.4.3, $d_f \approx 2.6$ at the percolating threshold, which agrees with previous numerical results [11]. With decreasing temperature, d_f rapidly rises towards 3, when the mean-field region is established. Almost all sites are then connected to the percolating cluster, (though not necessarily all bonds are open.) In the mean-field region, a continuum approximation gives

$$\rho_s(T) = \int_0^\infty dr P(r) \rho_s(r, T), \qquad (5)$$

where $P(r)dr$ is the probability that the radius of a channel lies between r and $r + dr$.
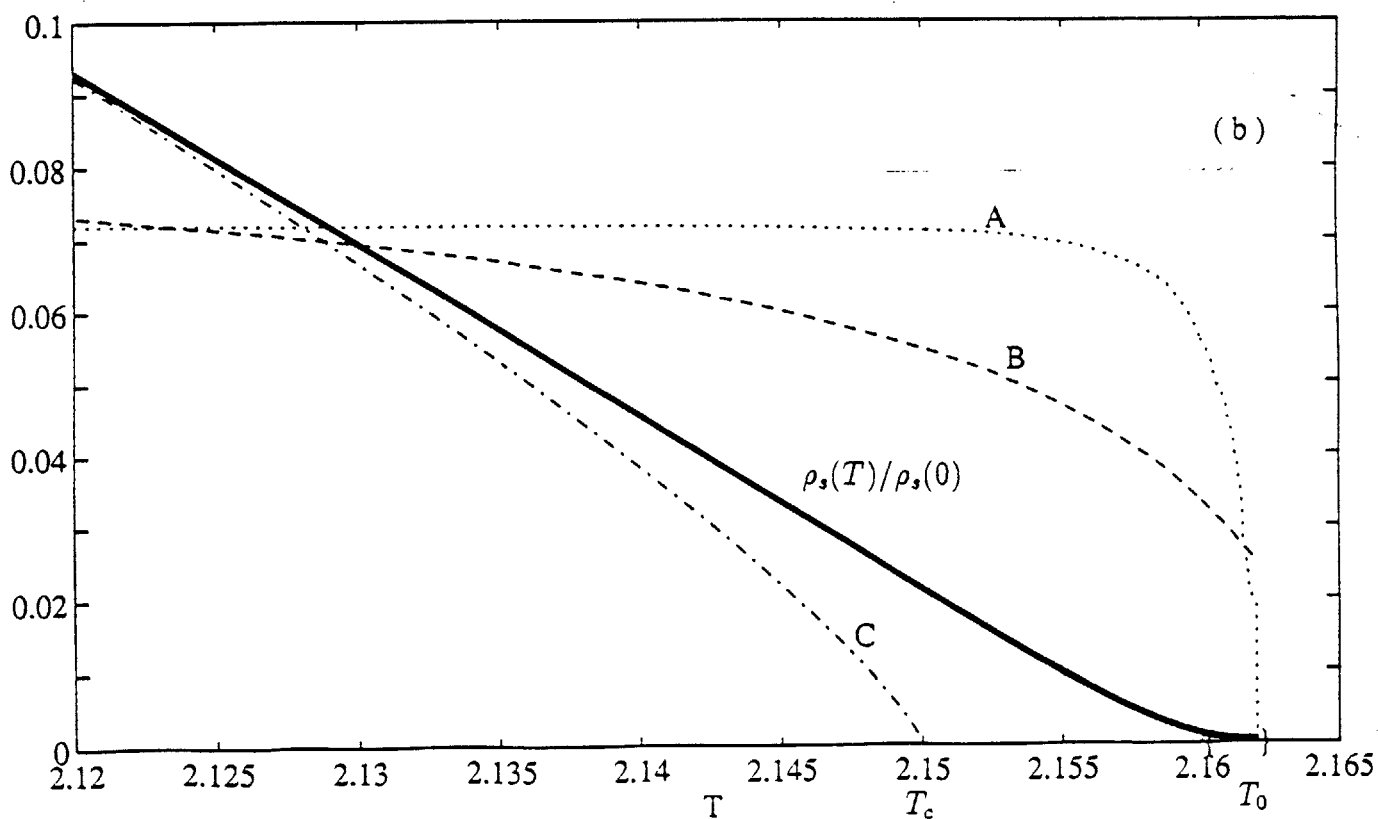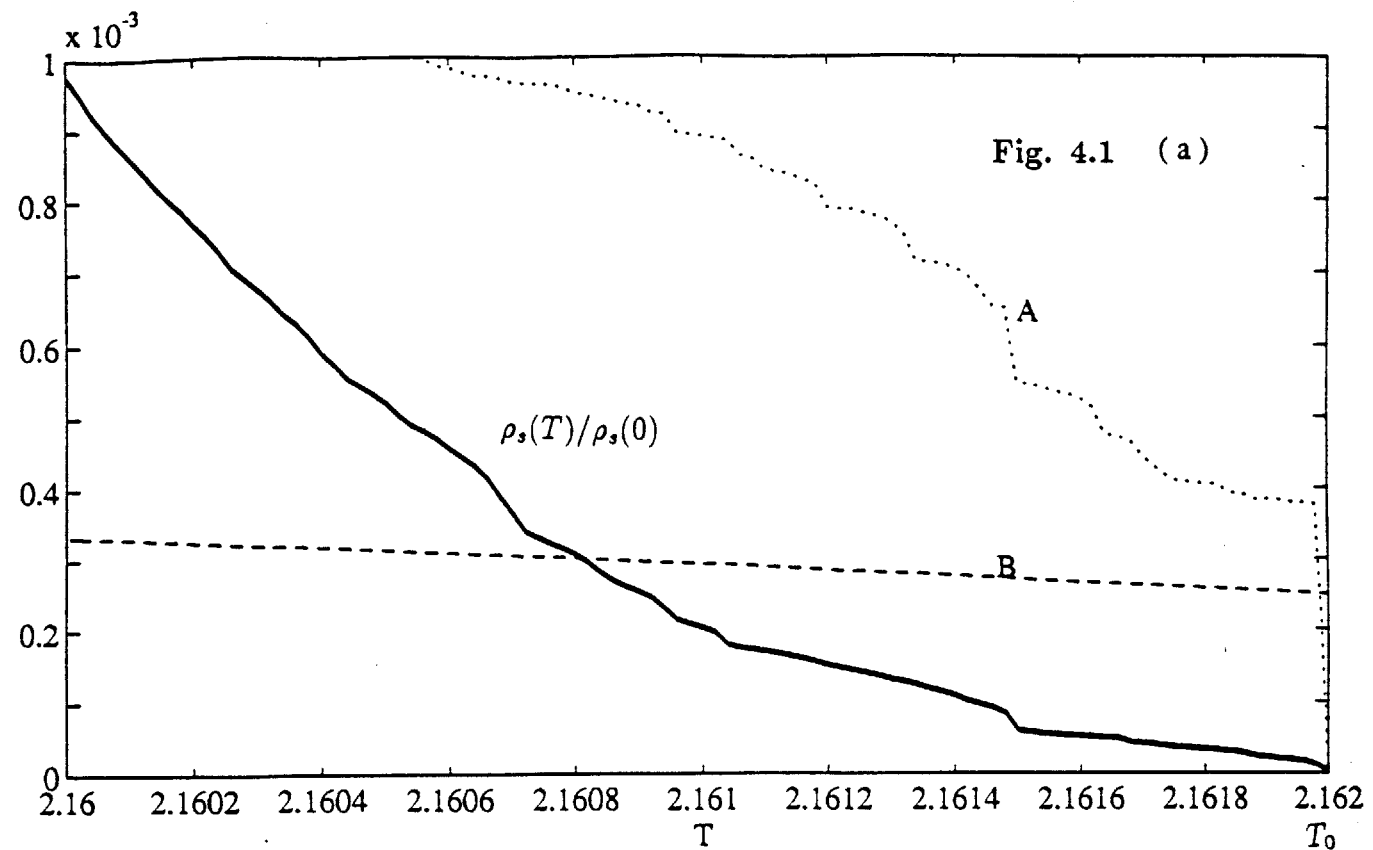
Panel (a) shows the superfluid density from the computer simulation as function of temperature, very near the percolation threshold. Curve A shows the percolating cluster size, and curve B shows the fraction of open bonds. Lattice size is 20^3, with a Gaussian distribution of bond radii. Panel (b) is a zoom-out from (a), whose temperature range is shown enclosed in curly brackets. The very beginning of the mean-field region now comes into view. Curve C is the power-law fit that determines ζ and T_c.
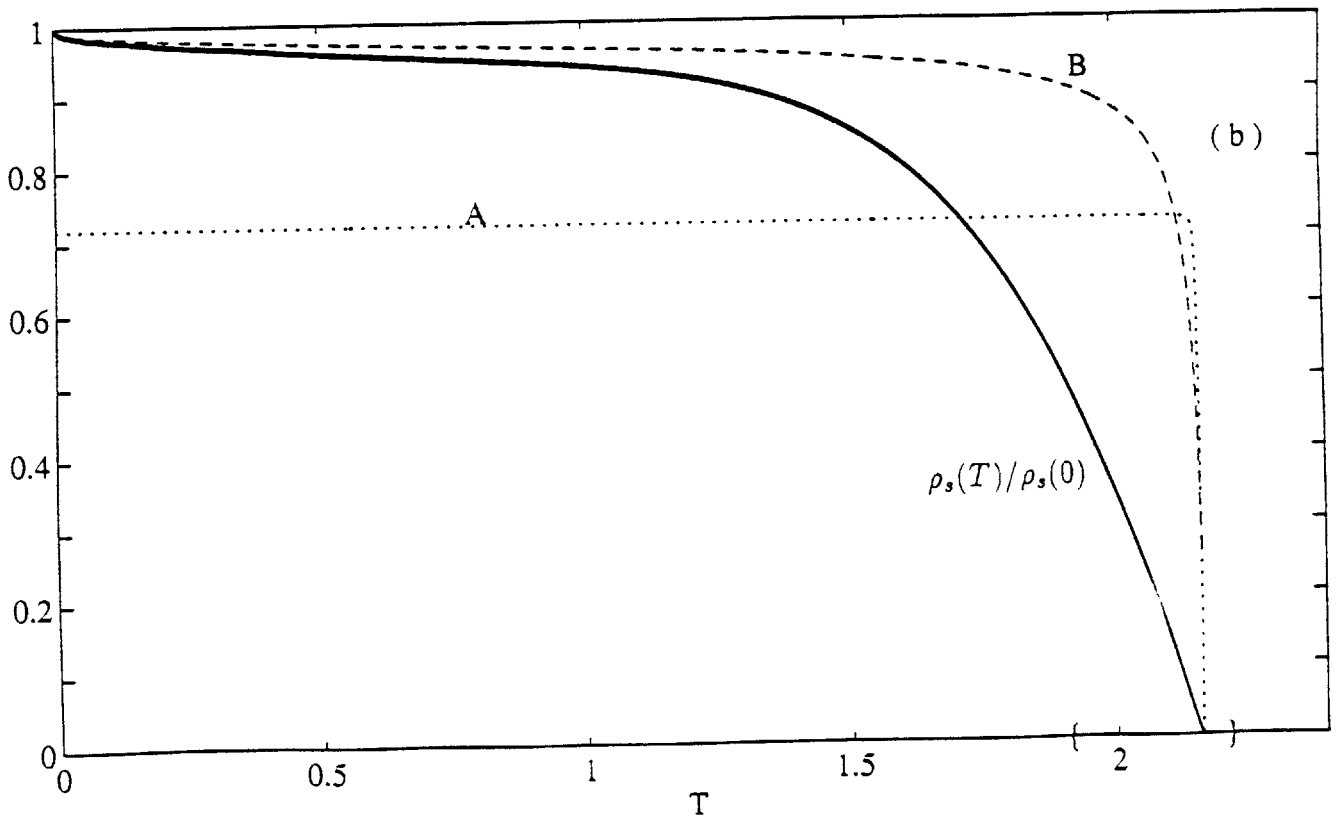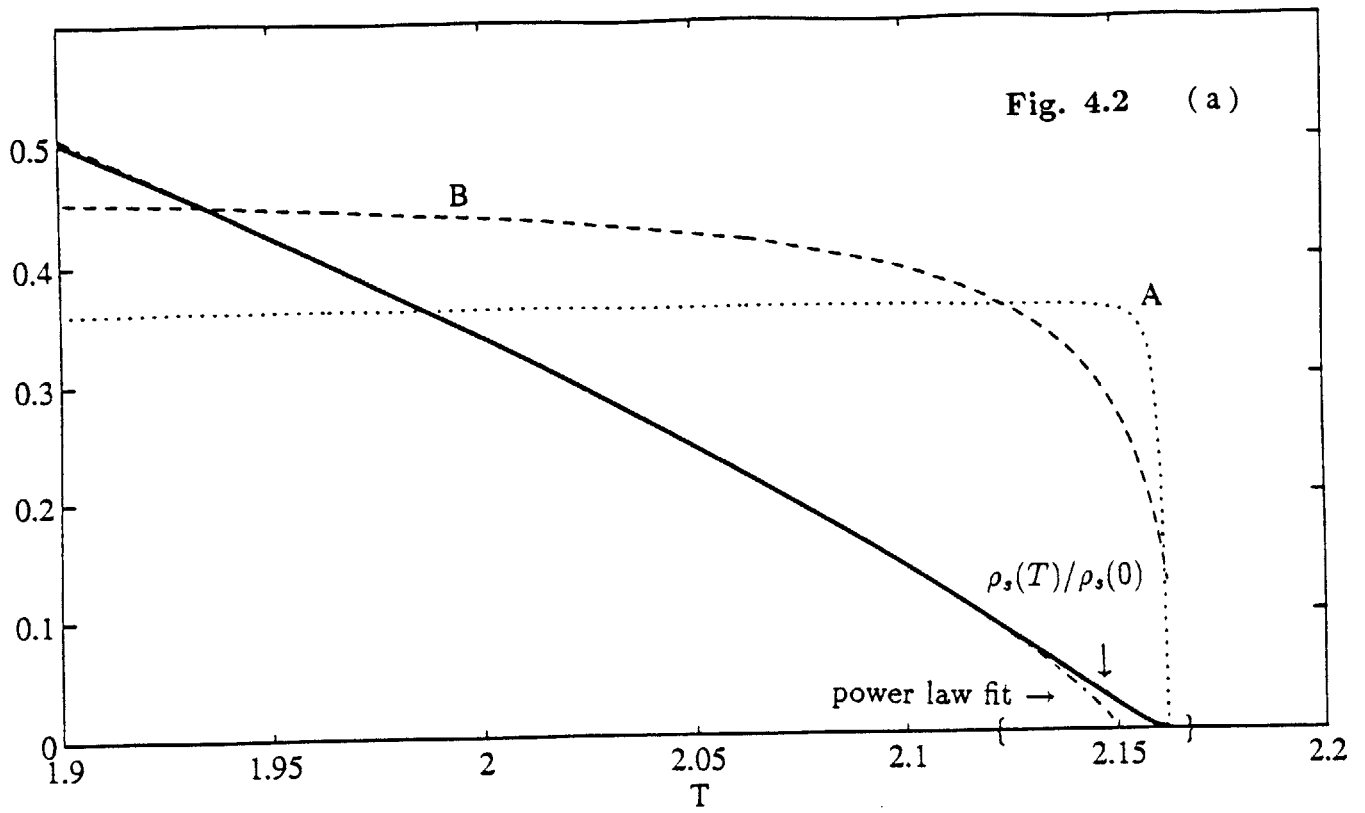
Panels (a) and (b) continue the zoom-out from Fig.4.1. The temperature interval covered in the previous region is enclosed in braces. In (a) the mean-region is fully visible, together with the power-law fit. In (b) the power-law fit becomes indistinct.

84
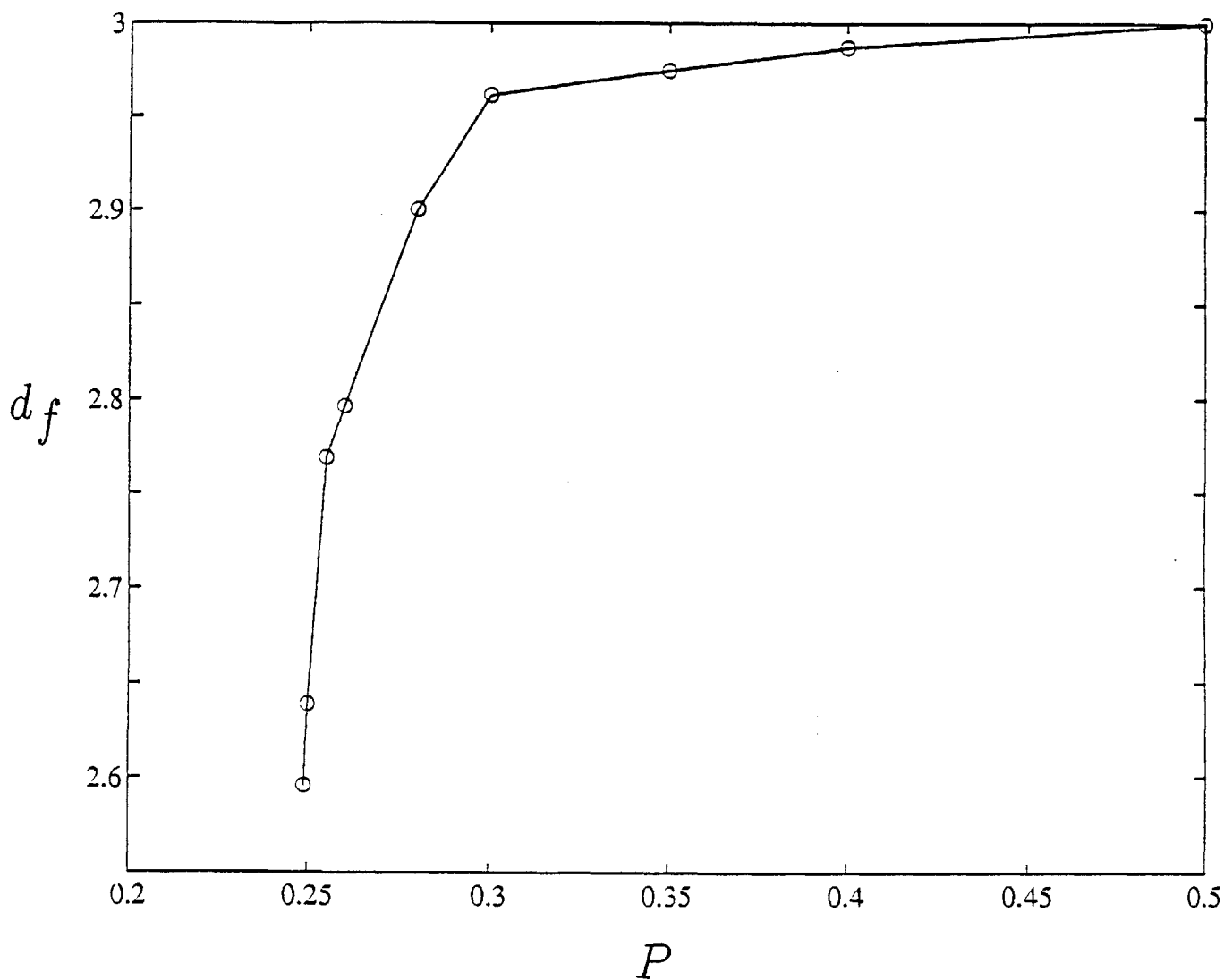
Fig. 4.3

Fractal dimension d_f of the percolating cluster as function of the fraction of open bonds p. The latter was given as a function of temperature in curve B of Fig.4.1a. The simulation was done in a 50^3 lattice.

We determine ζ by introducing an effective transition temperature T_c, plotting the computed superfluid density against $T_c - T$ in a log-log plot, and adjusting T_c until a straight line obtains for a range deem significant. The method involves subjective judgement, but it is precisely that used on the experimental data [10]. Since ζ is not associated with critical phenomena, there is no reason to expect it to have universality. It depends strongly on the distribution function of the radii. The discrepancy in the aerogel results between Refs.[2] and [4] might be due to differences in distribution functions. In Fig.4.4a, we plot ζ for a Gaussian distribution as a function of the width of the distribution. Fig.4.4b shows that for a uniform distribution, as a function of the upper cutoff. The observed values for Vycor, aerogel, and xerogel can all be reproduced.

Examples of the log-log plots used to determined ζ are shown in Fig.4.5, where we include three choices of the distribution function that can reproduce the experimental data for Vycor, aerogel, and xerogel, respectively. As for the true critical region, there are not enough experimental data to make a conclusive judgement. However, if we interpret the "rounding" of the power law fit observed in experiments as due to the perrcolation we can make a preliminary comparision. The result is shown in Fig. 4.6. As one can see, at least the experiment data do not rule out our theoretical prediction of the critical index 1.7.

In the following, we comment on the comparison with experimental data.

Vycor is known to have relatively uniform pore radii, which are small compared to channel lengths [1] [12]. The assumptions in our model are tailored for this case, and we can fit both ζ and the crossover region rather well. It is not surprising that ζ lies close to the bulk value, while T_c does not. In the extreme case where all pores sizes are exactly

the same, the percolation cluster would be saturated as soon as it occurs, and ζ would have the input bulk value. The transition temperature, however, would be depressed by the finite pore size.

.

Fig. 4.4 (a)

(b)
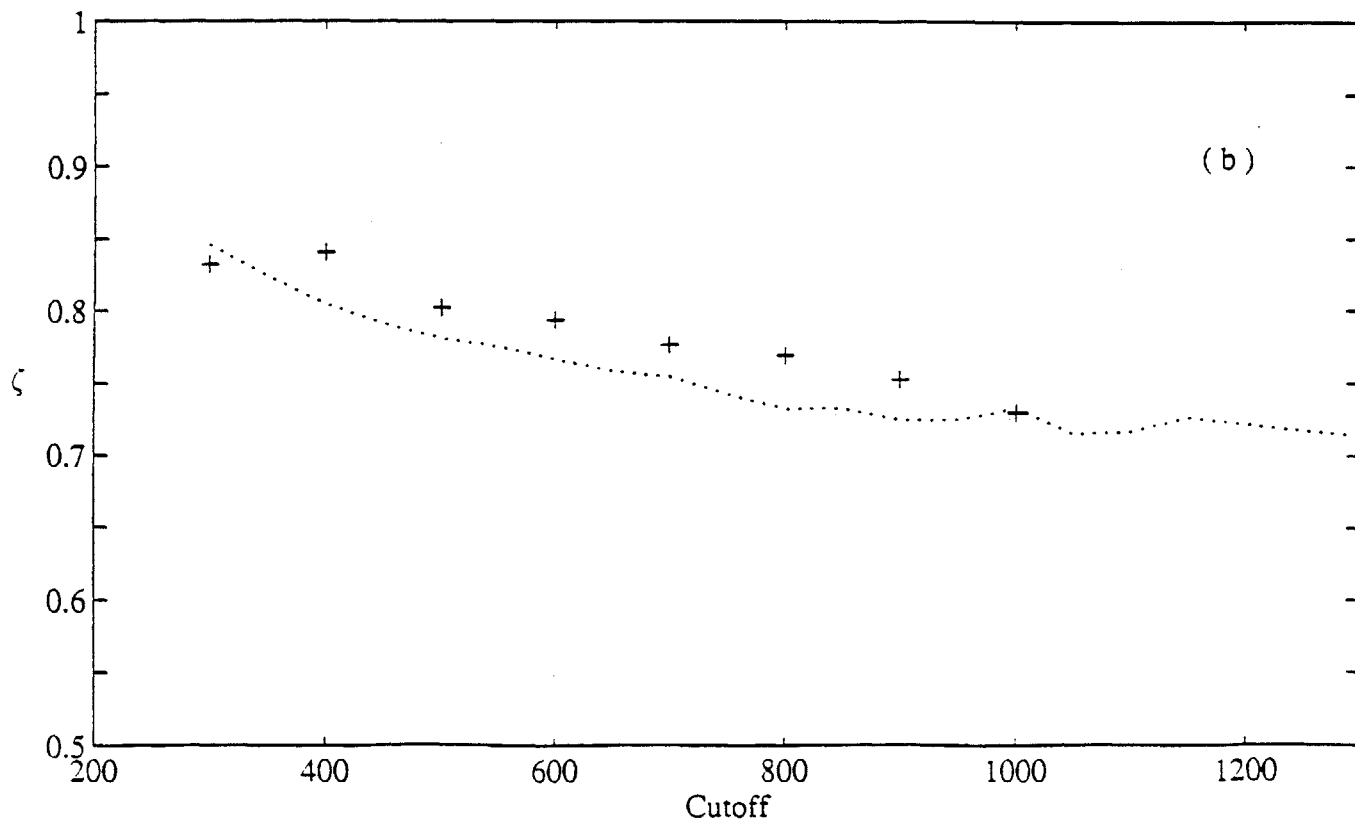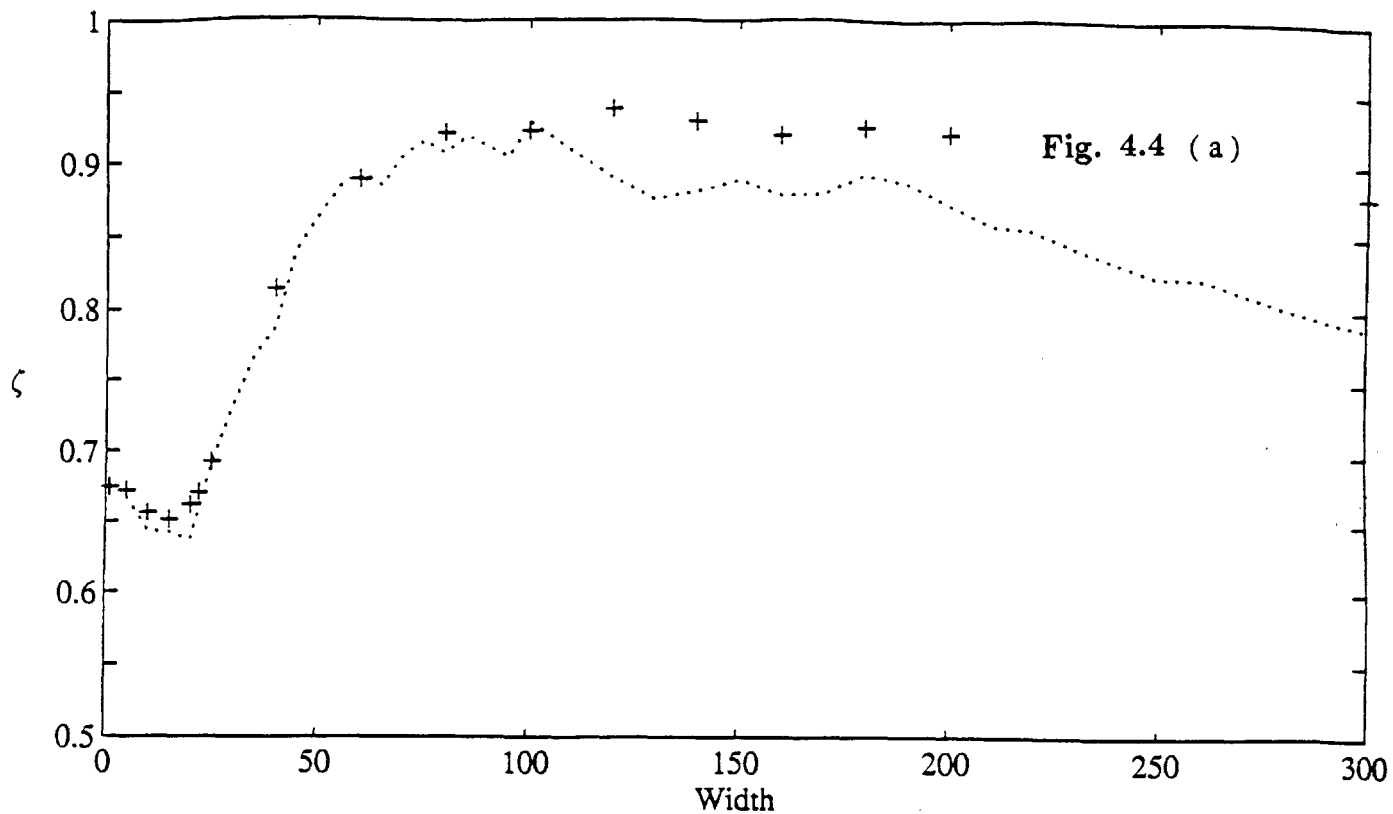
The effective exponent ζ as function of parameters that define the disordered medium. The crosses are from computer simulations, and the curves are obtained using the continuum approximation Eq.(5). In (a) the radius distribution is a Gaussian centered at 100 A. with variable width in Angstroms. In (b) the distribution is uniform from zero to a variable upper cutoff in Angstroms.
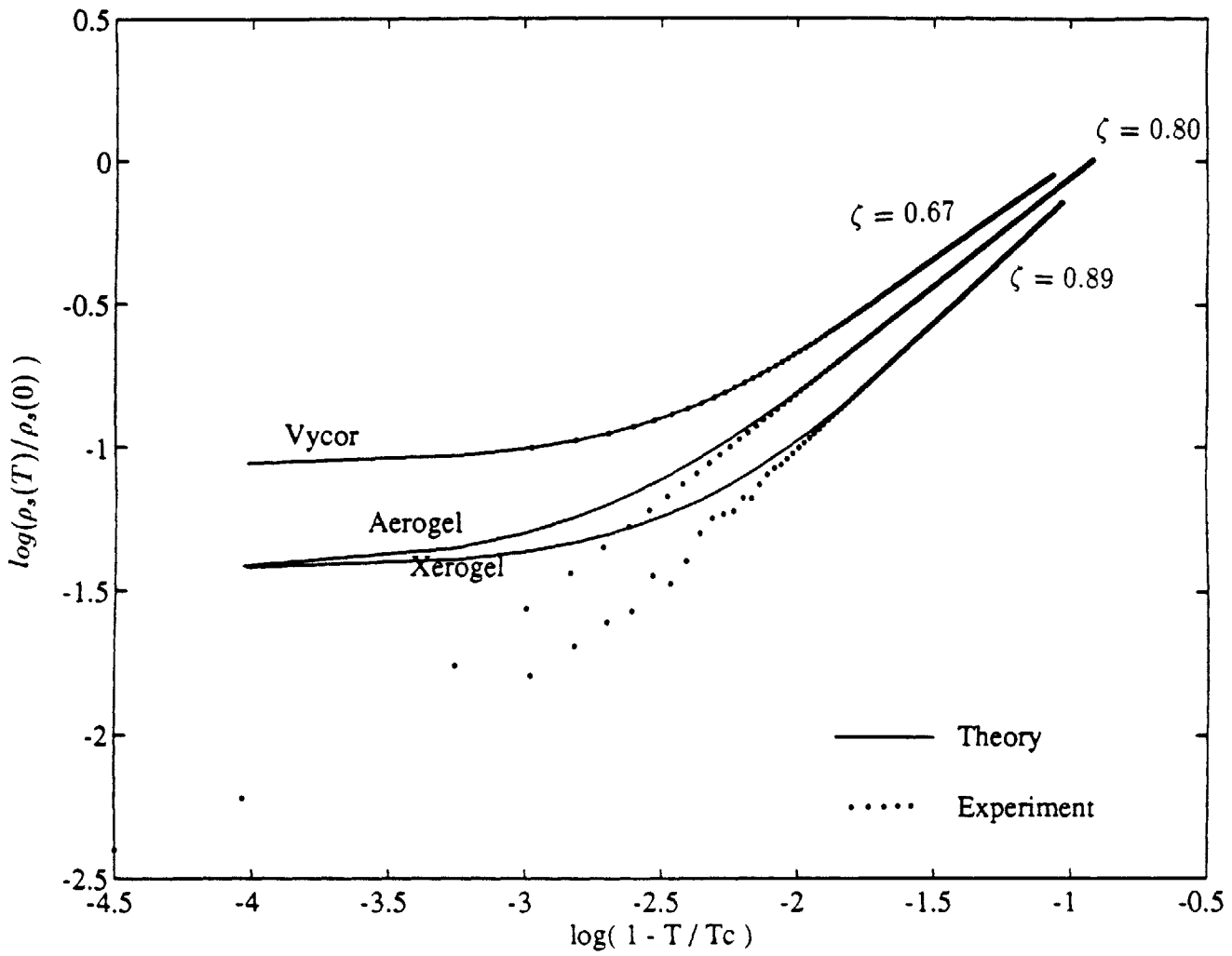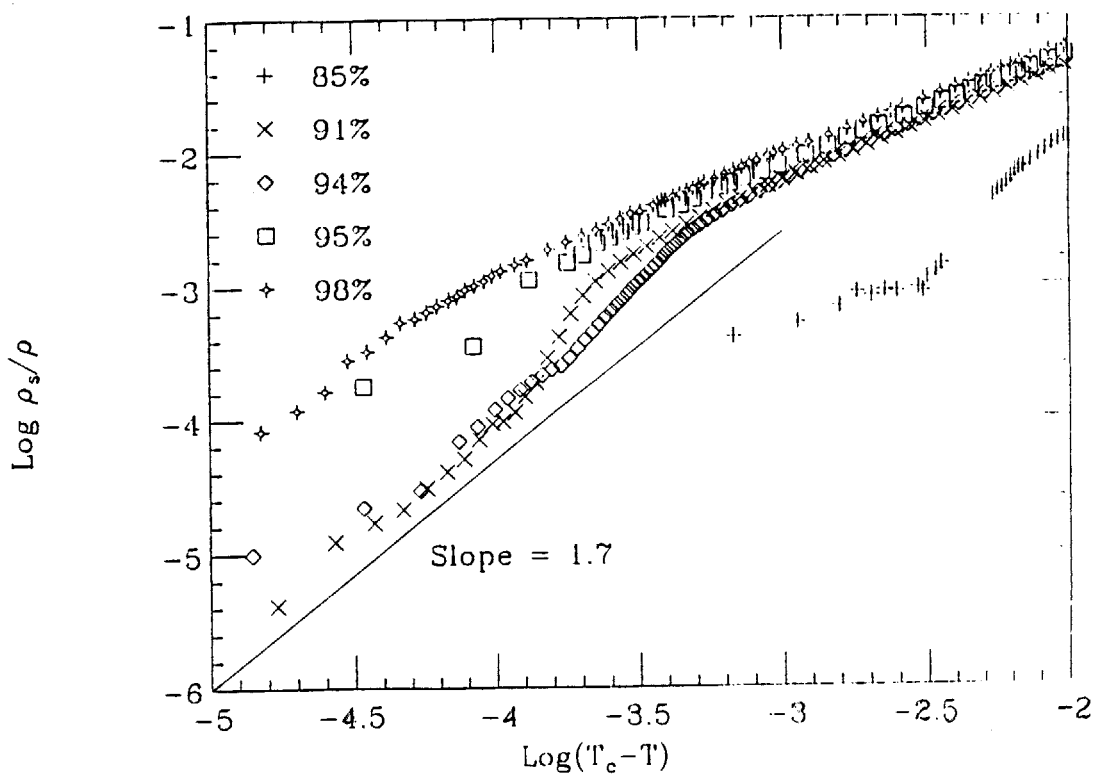
Fig. 4.5

Log-log plot of superfluid density against $T_c - T$, where T_c has been adjusted to yield the best straight line. The distribution functions are chosen to reproduce ζ. The curves have been displaced vertically relative to one another. for visual comparison of the slopes. The dots are experimental points read off the graphs in Ref.[2].

Fig. 4.6

The experimental data in the rounding region are shown with the theoretical prediction of critical index 1.7. Due to the fluctuation and the scarcity of the data it's very difficlut to make a conclusive judgements. Howeve, at least they do not conflict with each other apparently.

90

Aerogel has fractal structure, and the pores are not paticularly channel-like [13]. Our best shot is to choose a broad distribution of radii. Not surprisingly, this makes ζ different from the bulk value, but brings T_c closer to bulk value, because of the prevalence of large pores. Although ζ can be fit by adjusting the width of the distribution, the data shows a wider mean-field region.

Xerogel is essentially collapsed Aerogel, and has long channels along which the radius varies, because small offshooting branches have been pinched shut [14]. Again, we can fit ζ but not the extend of the mean-field region. A better model for this case might be to allow the channels to have segments of varying radii.

Further studies are needed to clarify the nature of the critical point, particularly concerning finite-size scaling, and effects of thermal fluctuations.

References

[1] For a comprehensive review see J.D. Reppy, J. Low Temp. Phys., **87**, 205 (1992).

[2] M.H.W. Chan, K.I. Blum, S.Q. Murphy, G.K.S. Wong, and J.D. Reppy, Phys. Rev. Lett. **61**, 1950 (1988).

[3] G.K.S. Wong, P.A. Crowell, H.A. Cho, and J.D. Reppy, Phys. Rev. Lett., **65**, 2410 (1990).

[4] N. Mulders, R. Mehrotra, L.Goldner, and G. Ahlers, Phys. Rev. Lett., **67**, 695 (1991).

[5] K.Huang and H.F. Meng, Phys. Rev. Lett. **69**, 644 (1992).

[6] R. Donelly, R. Hills, and P. Roberts, Phys. Rev. Lett., **42**, 75 (1979).

[7] W.H. Press, B.P. Flannery, S.A. Teukolsky, and W.T. Vettering, *Numerical Recipes*, (Cambridge University Press, Cambridge, England, 1986), Sec.17.5.

[8] J. Straley, Phys. Rev. **B15**, 5733 (1977).

[9] B. Josephson, Phys. Lett. **21**, 608 (1966).

[10] G.K.S. Wong, Ph.D. Thesis, Cornell Univeristy (1990).

[11] D. Stauffer and A. Aharony, *Introduction to Percolation Theory*, 2nd ed. (Taylor and Francis, London, 1992), p.10.

[12] K.I. Blum, Ph.D. Thesis, Cornell University (1989).

[13] *Aerogels: Proceedings of the First International Symposium*, J. Fricke, ed. (Springer-Verlag, Berlin, 1988).

[14] M.W. Shafer, D.D. Awscalom, J. Warnock, ans G. Ruben, J. Appl. Phys., **C1**, 5438 (1987).

Acknowlegements